This is the accepted manuscript (postprint) of the following article:
Najafi, M., & Eslami-Farsani, R. (2021). Design and characterization of a multilayered hybrid cored-sandwich panel stiffened by thin-walled lattice structure. *Thin-Walled Structures*, *161*, 107514.
https://doi.org/10.1016/j.tws.2021.107514

Design and characterization of a multilayered hybrid cored-sandwich panel stiffened by thin-walled lattice structure

Moslem Najafi, Reza Eslami-Farsani*

Faculty of Materials Science and Engineering, K. N. Toosi University of Technology, Tehran, Iran

* Corresponding author: eslami@kntu.ac.ir

Abstract

Low-density polyurethane (PU) foams have been commonly used for some structural purposes in marine applications. However, they have not been exploited as a structural core because of damage tolerance and durability concerns. The major drawbacks of sandwich panels having PU foam core are their poor mechanical properties and vulnerability to marine environmental conditions. Therefore, the present study aimed to contribute to enhancing both the mechanical properties and environmental durability of the traditional PU foam cored-sandwich panels through introducing a potentially suitable alternative. For this purpose, an innovative panel with a multilayered hybrid core consisting of agglomerate cork and PU foam was proposed which was orthogonally stiffened by a thin-walled lattice structure and sandwiched between two composite skins. To characterize the environmental durability and mechanical properties of this novel panel, a wide range of experimental tests including water immersion conditioning, three-point bending, edgewise and flatwise compression, quasi-static indentation, and high-velocity impact perforation were conducted. The sandwich specimens made of composite skins and PU foam core were also manufactured and tested for comparative purposes. Additionally, a nonlinear finite element (FE) analysis was also carried out and the numerical results were compared with the experimental data. The principal findings were that the proposed structural modifications caused a significant enhancement in all the studied mechanical and durability properties of PU foam-cored sandwich panels. It was also found that the FE model could predict load-displacement behavior of the studied sandwich panels under a variety of experimental conditions.

This is the accepted manuscript (postprint) of the following article:
Najafi, M., & Eslami-Farsani, R. (2021). Design and characterization of a multilayered hybrid cored-sandwich panel stiffened by thin-walled lattice structure. *Thin-Walled Structures*, *161*, 107514.
https://doi.org/10.1016/j.tws.2021.107514

Keywords: Multilayered hybrid cored-sandwich panel, Thin-walled lattice structure, Mechanical properties, Environmental durability, Finite element analysis

1. Introduction

Increasing the speed and dimensions of marine vessels are the most driving forces in the growing demand for lighter and stronger materials in the marine field [1]. Lightening weight provides excellent opportunities to have higher payload capacity, reduction in engine power corresponding to lower fuel consumption, higher operating speed, increased vessel stability, and lower life cycle costs [1-3]. Sandwich panels have received a great deal of attention in the marine sector due to their superior advantages such as high specific strength and stiffness, excellent corrosion resistance, good acoustic damping, and reasonable price [4-6]. A typical sandwich panel consists of a pair of thin, strong, and stiff skins supporting the bending moment as tensile or compression stresses [3,7]. The core as the thick and compliant part of the sandwich panel is responsible for supporting the shear stresses and stabilizing the skins against global and local instabilities [8,9]. Traditional marine sandwich panels mainly consist of composite skins and various types of light cores such as balsa wood [10,11], polyvinyl chloride (PVC) foams [12,13], polyurethane (PU) foams [14,15], etc.

Balsa wood has long been used in the construction of marine vessels due to its suitable characteristics e.g. low weight, remarkable stiffness, and high resistance against lateral impact loads compared to other similar cores with similar density [16-18]. However, high susceptibility to moisture absorption has hindered its widespread use in modern marine vessels. PVC foams are an attractive option in the construction of advanced marine structures. Although their closed-cell structure has successfully enhanced their water absorption resistance, on the other hand, it adversely affected the adhesion properties of the foam to composite layers. The core-skin debonding, especially in the bottom panel has limited their widespread use in marine structures [19,20]. Low-density PU foams have been used as non-structural part in marine vessels due to their noticeable features such as low price, good bonding with composite layers and ease of operation, shaping, and cutting. However, because of the substantial water absorption and relatively low mechanical properties, they have been never used directly in the sandwich bottom plate of marine vessels. It has been reported that salt spray and humid conditions can adversely affect the mechanical properties of PU foam-cored sandwich panels, especially for those having lower density foam core [21].

Regardless of the composite type either single-skin or sandwich panel, different types of internal members are necessarily used to improve the load-carrying capacity of marine vessels. However, the current secondary stiffening method is a time-consuming and costly process that significantly increases project execution time. The bottom plate fabrication is generally considered as the first step in the construction of composite vessels. Longitudinal and transverse stiffeners are then fitted on the precured bottom plate in two mutually perpendicular directions through the lamination process. Because of the low density of the unreacted polymer molecules, establishing a perfect and secure bonding between secondary structural elements and pre-cured structure is not always guaranteed. Debonding and detachment of stiffeners from the bottom plate are considered as consequences of the above-mentioned structural stiffening method. Such observations have been reported in previous studies literature. For example, the effect of the slamming loading on a part of the vessel's hull was investigated experimentally and numerically by Xue et al. [22]. The results showed that the stress concentration occurred near the conjunction of longitudinal and transverse stiffeners to the bottom plate. This region is particularly prone to delamination, detachment (join peel-off), and global failure in composite vessels. The design of stiffened panels in composite vessels, thus, requires special consideration to preserve the hull structure when deals with slamming loads.

Because of the relatively low bending stiffness of single-skin composite laminates, structural designers often must consider a large number of composite layers to meet the requirements of the marine regulations. Furthermore, poor impact tolerance of thin single-skin structures are often considered as one of the main challenges of structural designers in terms of comfortably and structural considerations. As an alternative, sandwich panels could solve some of the shortcomings of single-skin composite laminates. However, their inherent weaknesses i.e. relatively poor through-thickness compressive properties and susceptibility to delamination are the major obstacles to their wider use in the special structural application. Therefore, recently, the core strengthening methods have been developed using several innovative techniques such as stitching [23,24], z-pinning [25,26], shear key elements [27,28], and inserting the resin or composite walls/columns into the foam core [29, 30].

Lascoup et al. [31] found that through-thickness stitching of the core by glass fibers can improve the flexural behavior of PU foam core sandwich panels. In a research conducted by Yalkin et al. [32], it was found that the foam-cored sandwich panels with stitched cores performed structurally better than those have perforated cores filled with epoxy resin. Zheng et al. [33] produced a novel foam-based sandwich structure reinforced with partially-cured Z-pins made from T300/epoxy composite and reported that the use of composite Z-pins could significantly enhance the tensile strength, tensile modulus, and peeling strength of the sandwich panel. Taghizadeh et al. [34] reinforced PVC foam with three different composite corrugated core shapes, and experimentally studied the improvement of the compressive performance. It was found that the corrugated specimens filled with PVC foams possessed superior performance compared to those have no corrugation.

Besides the above-mentioned techniques, other innovative methods such as core hybridization have also been proposed to improve and optimize the behavior of the core behavior in sandwich panels. It was found that the use of hybrid cores in two categories of variable-density and variable-material can improve some mechanical properties of sandwich panels. Kaboglu et al. [35] studied the flexural and low-velocity impact properties of sandwich panels with a hybrid core consisting of different densities of PVC foam. The results showed that the use of a hybrid core with a designed pattern could enhance the flexural and impact performance significantly. Koohbor and Kidane [15] investigated the effect of density on energy absorption and load tolerance of PU hybrid foams. The results indicated that the use of a hybrid pattern instead of the conventional monolithic core led to improved energy absorption, enhanced load tolerance, and weight reduction of structure.

Previously, it was found that the low-density PU foams were not the typical choice in energy absorption applications such as slamming. As an environmentally sustainable and eco-friendly material, cork possesses good energy absorption performance as well as excellent water absorption resistance [36]. It is envisioned, therefore, that hybridization of PU foam with cork will provide a wide range of favorable features in terms of energy absorption, debonding resistance, high flexibility, and water absorption resistance (due to cork part), as well as low weight and low cost (due to PU foam). Regarding the high porosity of the cork surface, filling the resin in cork's pores may create the interlocking mechanisms, improving core-skin interfacial properties.

The main purpose of this study is to provide a practical solution to improve the weaknesses of traditional PU foam-based sandwich panels in terms of structural and durability properties while keeping the weight at its minimum. To achieve the desired goals, three strategies of through thickness stiffening of the core, multi-functional core hybridization, and improving the core-skin interfacial properties are considered in the design and construction process of the proposed sandwich panels. This paper introduces a sandwich panel in which the idea of water absorption resistant hybrid cores (agglomerated cork/PU foam) and lattice structures (epoxy/E-glass fiber composite) are used simultaneously for the first time. To investigate the environmental durability and structural performance of the resulting sandwich panels, the comprehensive testing program including the water immersion conditioning, three-point bending, edgewise compression, flatwise compression, indentation, and high-velocity impact perforation test was carried out. The traditional PU foam-cored sandwich specimens were also fabricated and tested as the control group for comparison purposes. Further, the three-dimensional (3-D) nonlinear finite element (FE) models were built to simulate the structural performance of the sandwich panels with the traditional and novel design.

2. Experimental procedure

2.1. Design concept

Here, the multilayered hybrid core was assembled from two thin layers of agglomerated cork bonded to a thick layer of PU foam as the external and internal parts of the core, respectively. It was expected that introducing agglomerated cork as the external surfaces exposed to environmental conditions can enhance water-resistance behavior, flexibility, and core-skin interfacial bonding strength of the sandwich panel. The idea of using agglomerated cork as an intermediate layer with moderate properties between the composite skins and PU foam probably has another beneficial contribution. It was envisioned that the gradual change of mechanical properties could prevent large interlaminar stresses at the core-skin interface where the delamination caused by the abrupt change in material properties is a common problem [37].

The composite lattice structure serves the dual purposes of connecting the top and bottom sandwich's skins and providing the support for core. In this way, the top and bottom skins are tightly integrated with the orthogonal lattice structure and there is practically no need to re-stiffening the structure with secondary structural elements. Conceptually and operationally, the lattice structure can prevent the core from premature crushing and delay delamination at skin-core interfaces.

A marine structural panel with the proposed sandwich structure under slamming pressure is schematically illustrated in Fig. 1. The difference in dimensions and spacing of the longitudinal structural members depends on how the slamming loads act non-uniformly on different parts of the hull structure. Obviously, a desirable structural scantling based on the design requirements of a real marine structure is necessary and achievable. In addition to the advantages mentioned above, the structure shown in Fig. 1 has potentially several technical and operational preferences as follows:

1. Simultaneous construction of the base plate and stiffeners can remarkably reduce project cost and execution time;
2. Stiffeners are tightly embedded inside the structure through the vacuum bagging method. Therefore, reduction in resin consumption corresponding to the elimination of re-stiffening process via the conventional method can lead to the significant weight lightening of the structure;
3. Filling the dead spaces between the stiffeners prevents the accumulation of water and other corrosive fluids and provides a flat surface in the upper part of the bottom panel. This is very beneficial in terms of structural and equipment arrangement design;
4. All the above-mentioned factors, especially weight loss, and structural performance enhancement, consequently lead to reduced fuel consumption and increased vessel speed.

This is the accepted manuscript (postprint) of the following article:
Najafi, M., & Eslami-Farsani, R. (2021). Design and characterization of a multilayered hybrid cored-sandwich panel stiffened by thin-walled lattice structure. *Thin-Walled Structures*, *161*, 107514.
https://doi.org/10.1016/j.tws.2021.107514

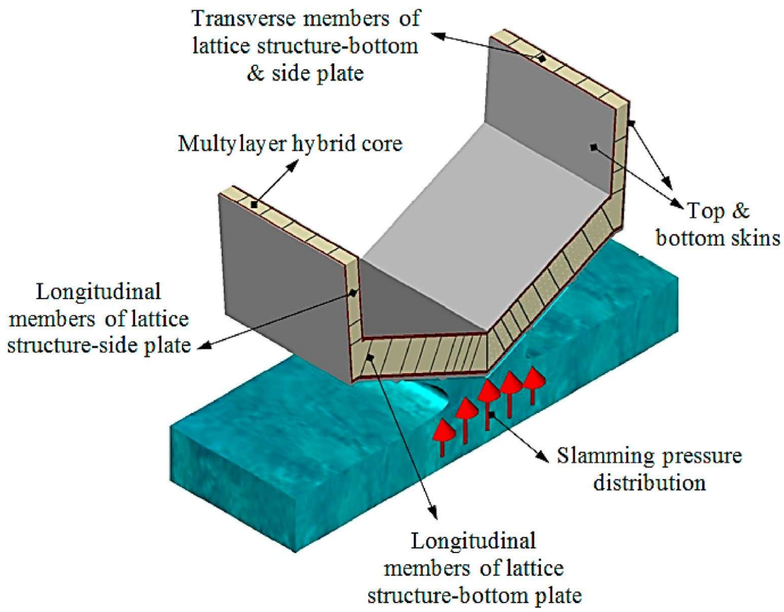

Fig. 1. Schematic of a marine structural panel made of the proposed sandwich structure under slamming pressure.

2.2. Materials and fabrication

The general specifications for two considered marine structural configurations are summarized in Table 1. Accordingly, the designation code of SP1 represents the common marine sandwich panel having epoxy/ glass fiber skins and a low-density PU foam core, which is referred as the baseline case. The configuration of SP2 is also the proposed sandwich panel with an agglomerated cork/low-density PU foam core stiffened orthogonally with a composite lattice structure and sandwiched by two epoxy/glass fiber composite skins. Due to the structural differences in the conceptual design of studied panels, it was an interesting challenge to design and fabricate both structures with almost the same weight. As can be seen from Table 1, the nominal areal weight of both configurations is approximately 8.41 kg/m^2 and the core thickness is the same in both cases and is equal to 25 mm.

Table 1. General specification of SP1 and SP2 configurations.

Specification	SP1	SP2
Panel type	Traditional sandwich panel	Lattice sandwich panels with multilayered hybrid core
Skin thickness (mm)	2.25	1.50
Stiffeners thickness (mm)	N/A	1
Core material	PU foam	Agglomerated cork/PU foam
Areal weight (kg/m^2)	8.42	8.41

Fig. 2 schematically shows the details of the fabrication process of SP2 sandwich panels. In this study, the multilayered hybrid core was built using a 2.5-mm-thick agglomerated cork sheet with 120 kg/m^3 density and PU foam with a thickness of 20 mm and 40 kg/m^3 density.

To fabricate the multilayered hybrid core, the agglomerated cork and PU foam sheets were cut into the required size (Fig. 2(a)). Both sides of the PU foam sheet were then completely covered with an epoxy adhesive (Araldite 2011/AB), and two sheets of agglomerated cork were bonded to its both sides. This assembly was then placed under the gentle pressure for 1 day (Fig. 2(b)) and eventually cut into the cubes with dimensions of 25 × 25 × 25 ± 1 mm as shown in Fig. 2(c).

The panel's bottom skin was made from six plies of a bi-directional woven E-glass fabric (200 g/m^2) and a two-component 828 epoxy resin supplied by Kumho P&B Chemicals, South Korea (Fig. 2(d)). Subsequently, the multilayered hybrid cubes were orderly positioned adjacent to each other on the above-mentioned composite plate as shown in Fig. 2(e). Two plies of E-glass fabrics were then cut into the same-size strips (Fig. 2(f)), impregnated with resin (Fig. 2(g)), and temporarily laid-up on either face of a certain cube (Fig. 2(h)). This process was repeated for two adjacent cubes until all impregnated plies were embedded between all cubes. In this step, the excess resin inevitably sagged on the bottom plate which is favorable for better bonding of lattice structure to the base plate.

Following that, the peel ply (release fabric), breather, and vacuum bag were placed over the assembled structure, respectively. The mold perimeter was then completely sealed by the mastic sealant and exposed to air evacuation provided by a vacuum pump as shown in Fig. 2(i). After curing at room temperature, the vacuum bag, breather, and peel ply were entirely removed from stiffened hybrid core and its upper surface was gently ground and cleaned (Fig. 2(j)). As the final stage of fabrication, the top skin of the sandwich panel was produced by lamination of epoxy/ glass fiber layers over the stiffened multilayered hybrid core (Fig. 2(k)). A manufactured SP2 specimen can be seen in Fig. 3.

The traditional sandwich panel namely SP1 with 25 mm monolithic PU foam (40 kg/m^3 density) and the same above-said composite skins was also prepared for comparative purposes. To obtain the same weight for two panels, the nine epoxy/E-glass plies were necessarily used to fabricate the skins of the SP1 panel. Fig. 4 graphically represents the structural parameters of two types of small-scale marine structural configuration.

This is the accepted manuscript (postprint) of the following article:
Najafi, M., & Eslami-Farsani, R. (2021). Design and characterization of a multilayered hybrid cored-sandwich panel stiffened by thin-walled lattice structure. *Thin-Walled Structures*, *161*, 107514.
https://doi.org/10.1016/j.tws.2021.107514

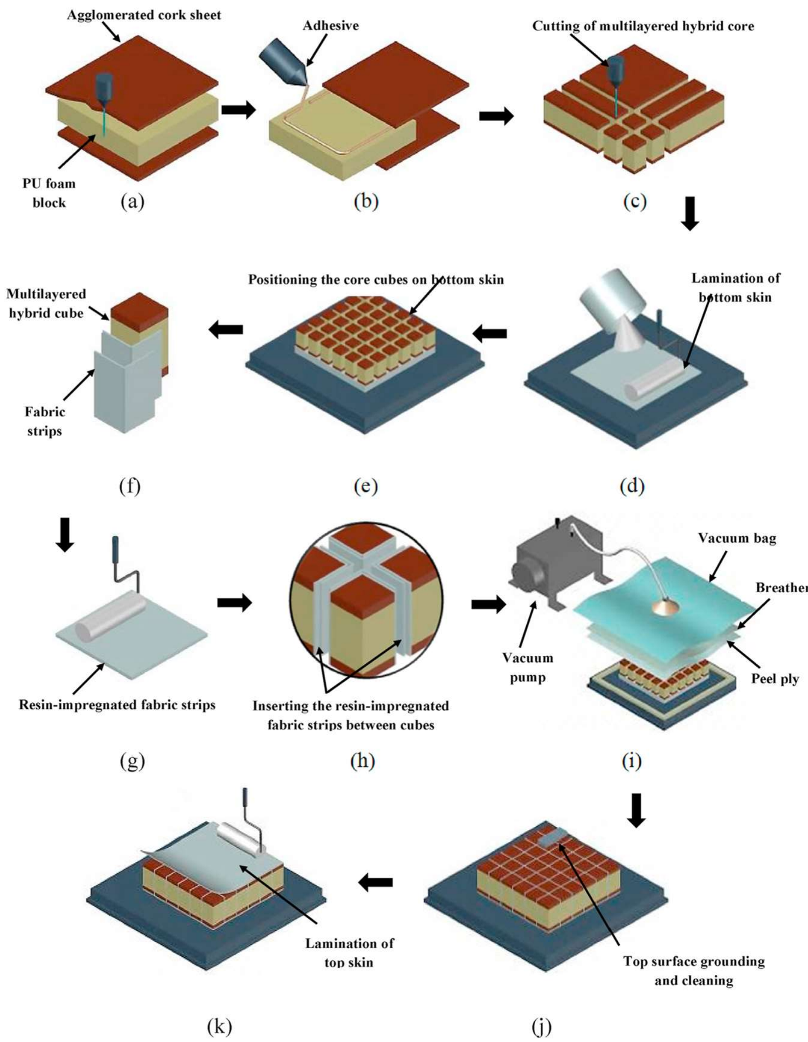

Fig. 2. Schematic of the manufacturing process of SP2 sandwich panel based on multilayered hybrid core and thin-walled lattice structure.

This is the accepted manuscript (postprint) of the following article:
Najafi, M., & Eslami-Farsani, R. (2021). Design and characterization of a multilayered hybrid cored-sandwich panel stiffened by thin-walled lattice structure. *Thin-Walled Structures*, *161*, 107514.
https://doi.org/10.1016/j.tws.2021.107514

Fig. 3. Photograph from a typical SP2 specimen.

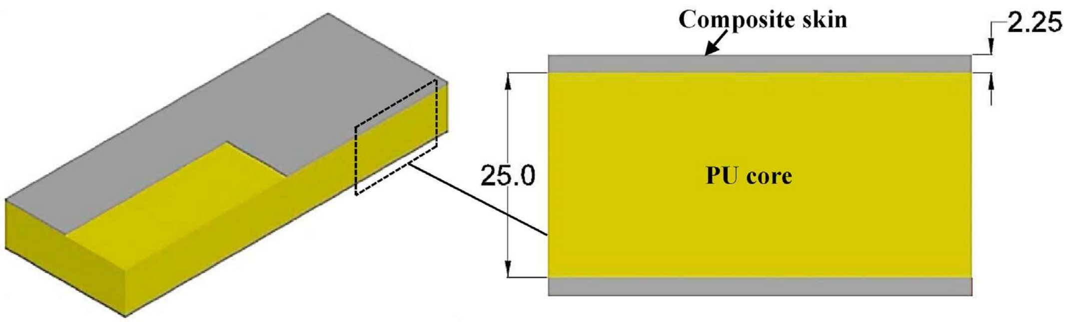

(a)

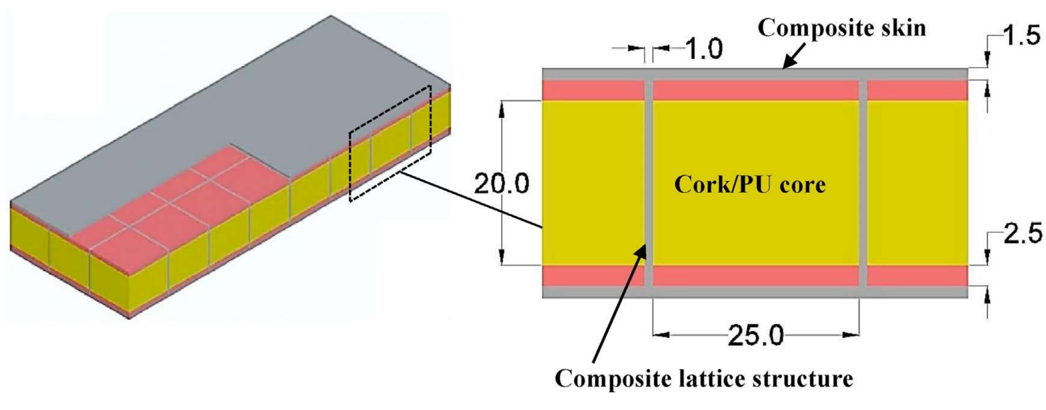

(b)

Fig. 4. Schematic illustration of marine structural configurations for (a) SP1, (b) SP2 specimens (all dimensions are in mm).

2.3. Materials tests

2.3.1. Mechanical testing of the constituent materials

Determining the mechanical properties of constituent materials is an essential step for the numerical simulation of structural behavior. Therefore, the required compressive properties of PU foam and tensile properties of epoxy/glass fiber composite were experimentally determined. However, due to the thinness of agglomerated cork sheets, its mechanical properties were inevitably extracted from the product datasheets [38]. The compression tests, according to ASTM D1621 standard [39], were conducted on a universal testing machine Hounsfield (Model H25KS, UK) to characterize the compressive properties of PU foam. The cubic PU foam specimens with an overall dimension of 60 × 60 × 50 mm^3 (length × width × thickness) were loaded in the parallel direction to the foam rise, at a constant cross-head speed of 3 mm/min, the temperature of 23 ± 2 °C and relative humidity (RH) of 51 ± 3% as shown in Fig. 5(a). The ASTM D3039/D3039 M standard [40] was performed to determine the tensile properties of the composite skins and lattice structure. The tension test was conducted on the above-mentioned testing machine with a cross-head speed of 2 mm/min at the temperature of 22 ± 2 °C and 51% RH (Fig. 5(b)). The dimensions of the rectangular tensile specimens were 250 × 25 × 2.5 mm^3 (length × width × thickness) according to the standard recommendations.

This is the accepted manuscript (postprint) of the following article:
Najafi, M., & Eslami-Farsani, R. (2021). Design and characterization of a multilayered hybrid cored-sandwich panel stiffened by thin-walled lattice structure. *Thin-Walled Structures*, *161*, 107514.
https://doi.org/10.1016/j.tws.2021.107514

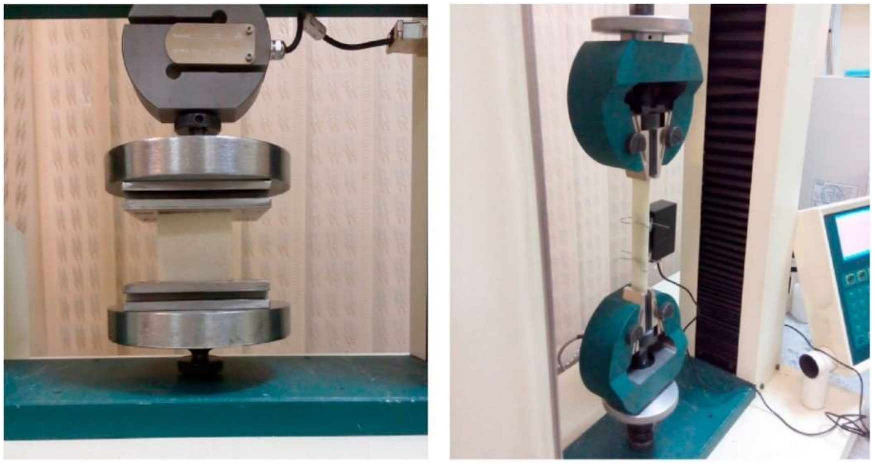

(a) (b)

Fig. 5. Test setup for (a) PU foam compressive specimen, (b) Composite tensile specimen.

2.3.2. Water absorption conditioning

The water absorption behavior of core materials was determined via the water immersion test. A set of specimens with nominal dimensions of 25 × 25 × 2.5 mm^3 (length × width × thickness), including PU foam with 6 open edges (designated as PU), PU foam with 2 open edges and 4 sealed edges (PU/S) and multilayered agglomerated cork/PU foam with 2 open edges and 4 sealed edges (PU/C/S) were prepared for environmental aging tests. The considered edges were coated by a thin layer of epoxy resin to reduce the water penetrate from these sealed edges. The specimens were then completely immersed in a tank containing water for 100 days. Because all specimens were less dense than water, they were naturally floated on the water surface. Therefore, to complete immersion of the specimens during the aging process, plastic loose nets were placed on the specimens to ensure the water could penetrate uniformly from all directions. The change in weight as a function of time was continuously recorded. For this purpose, the specimens were periodically removed from the water tank and, after drying by a moisture-absorbing towel, weighed by a high-precision digital scale. The percentage of water absorption (M_t) was calculated by equation (1):

This is the accepted manuscript (postprint) of the following article:
Najafi, M., & Eslami-Farsani, R. (2021). Design and characterization of a multilayered hybrid cored-sandwich panel stiffened by thin-walled lattice structure. *Thin-Walled Structures*, *161*, 107514.
https://doi.org/10.1016/j.tws.2021.107514

$$M_t(\%) = (\frac{W_t - W_0}{W_0}) \times 100 \quad (1)$$

where W_t is the specimen weight at time t and W_0 is the initial weight of the specimen.

2.3.3. Sandwich panels tests

A series of quasi-static tests including flexural test, flatwise and edgewise compressive test, as well as concentrated quasi-static indentation test was performed at RH 49 ± 3% and 24 ± 2 °C using a universal testing machine, Hounsfield (Model H25KS, UK) equipped with a 25 kN load cell. For each test, three specimens of each configuration category were prepared and the average results were reported. Geometrical dimensions and number of constructive stiffeners of lattice structure for SP2 test specimens are tabulated in Table 2. Although the SP1 specimens have no internal stiffeners, their main dimensions were designed to be equal to the SP2 specimens.

Table 2. Geometrical dimensions and scantling of SP2 specimens.

Specification	Length (mm)	Width (mm)	No. of longitudinal stiffeners	No. of transverse stiffeners
Flexural test	207	77	7	2
Flatwise compressive test	77	77	2	2
Edgewise compressive test	77	77	2	2
Indentation test	51	51	1	1
High-velocity impact perforation test	103	103	3	3

a) Flexural test

The wave-induced bending moments such as hogging and sagging are often considered as the most common loading conditions that marine vessels experience during their service-life. Thus, flexural testing was employed in this study to demonstrate the effectiveness of the currently proposed design to enhance the structural performance of PU foam core sandwich panels. In this way, the three-point bending (3 PB) tests were performed according to the

ASTM C393/C393 M standard [41]. The nominal dimension of the rectangular flexural specimens was 207 × 77 mm^2 (length × width). The span length of 157 mm and a cross-head speed of 6 mm/min were considered for two types of 3 PB specimens. The experimental set-up for the 3 PB test and the SP1 specimen under flexural loading is illustrated in Fig. 6(a).

b) Flatwise compression test

The low-velocity impact of the hull with waves, commonly known as slamming is one of the main sources of compressive stress generation in marine vessels. The flatwise compressive tests were therefore conducted to evaluate the compressive behavior of studied materials along the outof-plane direction. As shown in Fig. 6(b), the square specimens with dimensions of 77 × 77 mm^2 were compressed at a cross-head speed of 0.5 mm/min, according to the ASTM C365/C365 M standard [42].

c) Edgewise compression test

Sandwich panels are widely used in compressive structural members of marine vessels such as pillars, sides, as well as watertight and nonwatertight bulkheads. However, when the load is increased to an excessively high value, the compressive structural element may exhibit core-skin debonding and/or core crushing which significantly could reduce the load-carrying capacity of the structure. Edgewise compression tests were therefore considered to evaluate the adequacy of the studied sandwich materials in terms of load-carrying capability in the direction parallel to the sandwich skins plane. The dimensions of the edgewise compression test specimens were the quite same with the compression flatwise compressive test (Fig. 6(c)). The square sandwich specimens were tested under compressive loading at a cross-head speed of 0.5 mm/ min, as per recommendations of ASTM C364 Standard [43].

This is the accepted manuscript (postprint) of the following article:
Najafi, M., & Eslami-Farsani, R. (2021). Design and characterization of a multilayered hybrid cored-sandwich panel stiffened by thin-walled lattice structure. *Thin-Walled Structures*, *161*, 107514.
https://doi.org/10.1016/j.tws.2021.107514

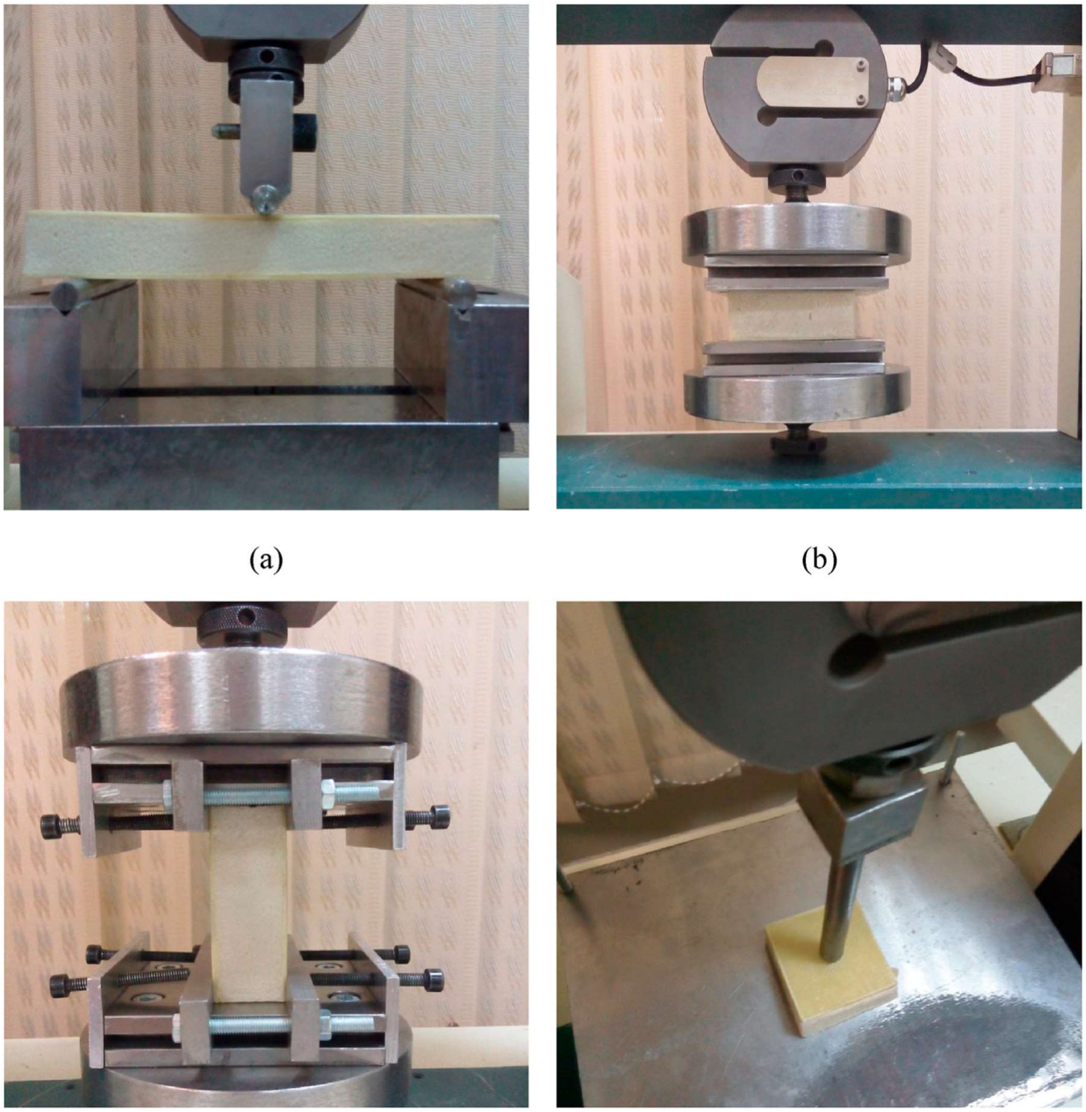

(a) (b) (c) (d)

Fig. 6. Mechanical tests conducted on SP1 specimen: (a) Three-point bending, (b) Flatwise compression, (c) Edgewise compression, (d) Concentrated quasi-static indentation.

d) Concentrated quasi-static indentation test

The marine sandwich structures are generally susceptible to localized point loads such as the collision with rocks, floating debris, falling objects, and grounding [12,36]. Since such events, even at low-velocity regime (or quasi-static conditions) can seriously threaten the safety and integrity of the structure, evaluating the damage characteristics of marine sandwich panels is therefore an essential step in marine structural design. Damage resistance properties of two types of sandwich systems were characterized according to the ASTM D7766/D7766 M standard [44] recommendations. For this purpose, the square specimens with dimensions of 51 × 51 mm^2 were placed on a flat rigid support which was mounted in the lower head of the testing machine. The concentrated quasi-static compressive load was then carried out at the center of specimens at a cross-head speed of 1.25 mm/min as shown in Fig. 6(d). The hemispherical indenter head had a diameter of 12 mm.

e) High-velocity impact perforation test

A single-stage light gas gun apparatus equipped with a gas storage vessel, gun barrel, solenoid valve, velocity sensors, capture chamber, and specimen fixture was used to determine the high-velocity impact perforation resistance of the sandwich specimens. Square targets with dimensions 103 × 103 mm^2 were edge clamped using eight wing nuts onto the steel fixture, having 100 × 100 mm^2 square aperture, as shown in Fig. 7(a). The targets were located 450 mm far from the tip of the gun barrel. The hemispherical nosed projectiles made of aluminum alloy 7075 with 26.7 g weight and 21.70 mm diameter (Fig. 7(b)) were launched at the incident velocity of 130 m/s to the center of targets, in which full perforation on SP1 specimens definitely occurred.

This is the accepted manuscript (postprint) of the following article:
Najafi, M., & Eslami-Farsani, R. (2021). Design and characterization of a multilayered hybrid cored-sandwich panel stiffened by thin-walled lattice structure. *Thin-Walled Structures*, *161*, 107514.
https://doi.org/10.1016/j.tws.2021.107514

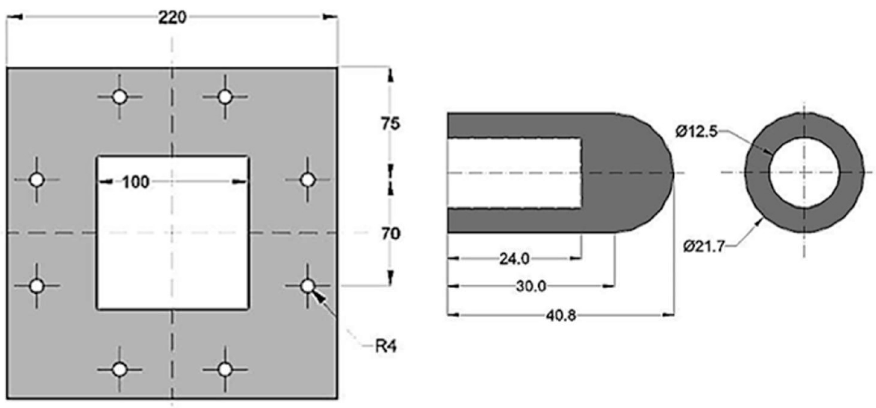

(a) (b)

Fig. 7. (a) Details of the clamping arrangement, (b) Geometries and dimensions of the hemispherical nosed projectile used during high-velocity impact perforation testing (all dimensions are in mm).

3. Finite element analysis

To evaluate the structural behavior of studied sandwich panels, the nonlinear 3-D FE analysis was conducted by commercial software package ANSYS. All of the sandwich constituents including agglomerated cork, polyurethane foam, and composite parts were meshed using 3-D hexahedron element (Hex 20) elements. This element is a high-order element having twenty nodes with three translational degrees of freedom (DOFs) at each node. Since neither visible primary defects at the core-skin interface nor delamination were observed during the elastic phase of experimental testing, the core-skin interface was assumed to be perfectly bonded in FE analysis.

Since the main purpose of numerical simulation was a versatile comparative study on design concepts of two structural configurations, some material-related simplifications were considered. Material properties obtained from the experimental tests were assigned to the sandwich constituents. Accordingly, an orthotropic material model was used for describing the elastic behavior of composite skins and lattice structure, while the agglomerated cork was defined as isotropic materials. The multilinear isotropic hardening model was also utilized to simulate the elastic-plastic behavior of PU foam. To prevent the common numerical errors caused by the bonding of thin skins to a thick core, the fine and uniform mesh has been used as much as possible, as shown in Fig. 8.

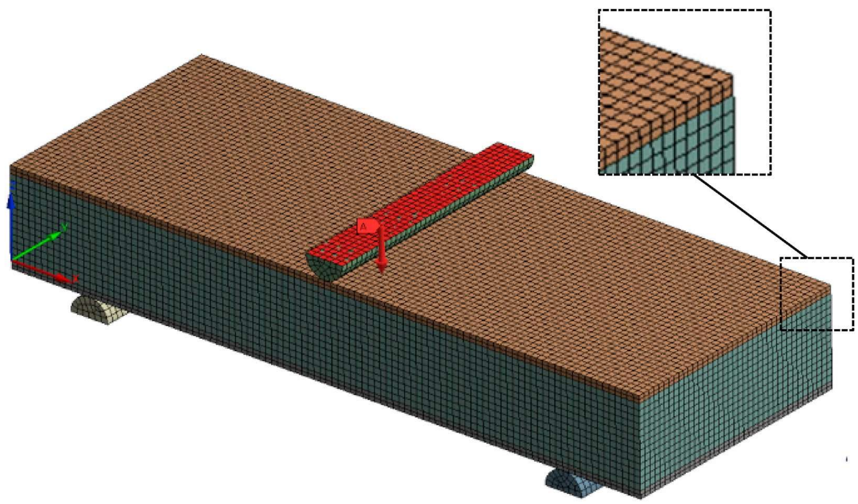

Fig. 8. Meshing and loading of the SP1 FE model.

4. Results and discussion

4.1. Material characterization

4.1.1. Constituent materials characterization

Fig. 9(a) presents the average compressive stress-strain curve for the PU foam cubic specimens. This curve exhibits a linear elastic behavior to material yield point at average stress of 0.20 MPa, followed by an extended flat plateau (between 10 and 65% strain) terminating in a densification region (above 65% strain). Young's modulus of PU foam was defined as the slope of the linear portion of the stress-strain curve, which was an average value of 7.22 MPa.

Fig. 9(b) illustrates the typical stress-strain curve following the tensile test on the epoxy/glass fiber composite laminates. The figure indicates a relatively linear behavior under tensile loading up to the fracture load, which can be attributed to the brittle nature of this type

This is the accepted manuscript (postprint) of the following article:
Najafi, M., & Eslami-Farsani, R. (2021). Design and characterization of a multilayered hybrid cored-sandwich panel stiffened by thin-walled lattice structure. *Thin-Walled Structures*, *161*, 107514.
https://doi.org/10.1016/j.tws.2021.107514

of composite laminates. The tensile modulus and ultimate tensile strength of tested composite laminates were defined to be the average values of 9890 MPa, and 224 MPa, respectively.

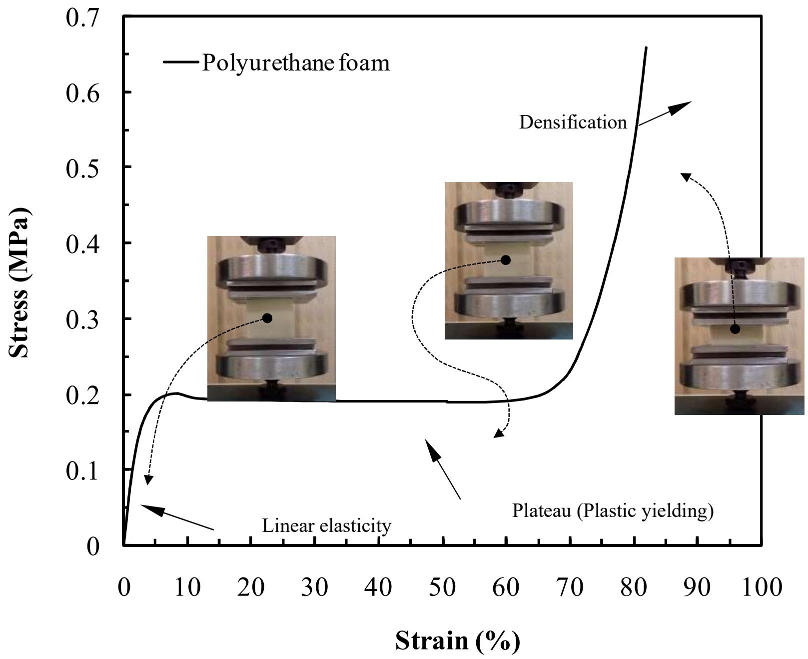

(a)

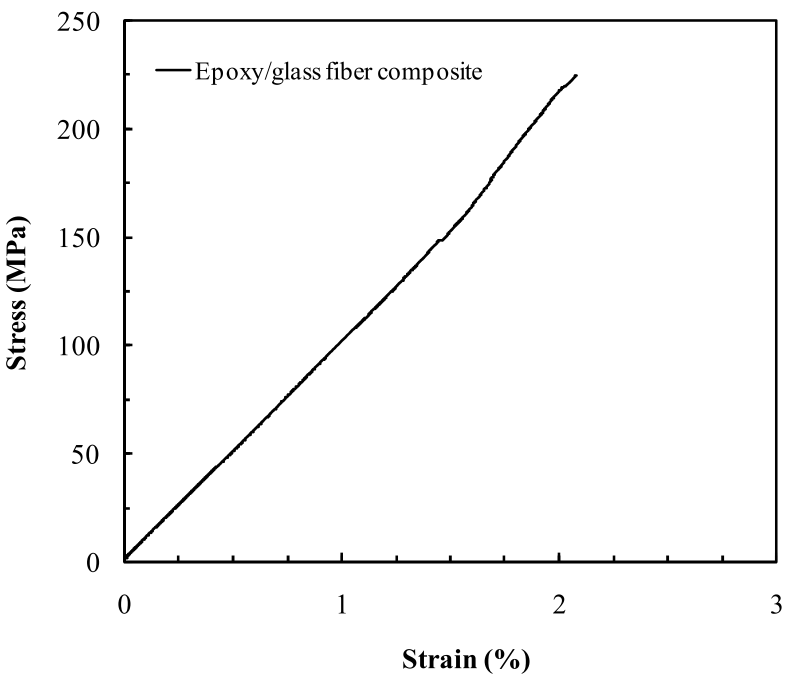

(b)

Fig. 9. Typical stress-strain curves for (a) 40 kg/m^3 PU foam in the uniaxial compression test, (b) Epoxy/glass fiber composite laminate under tension test.

This is the accepted manuscript (postprint) of the following article:
Najafi, M., & Eslami-Farsani, R. (2021). Design and characterization of a multilayered hybrid cored-sandwich panel stiffened by thin-walled lattice structure. *Thin-Walled Structures*, *161*, 107514.
https://doi.org/10.1016/j.tws.2021.107514

The material properties for the epoxy/glass fiber composite laminate, cork and PU foam are tabulated in Table 3. Accordingly, the Young's modulus $E_1 = E_2$ for composite laminate was directly derived from the experimental data. Since the composite laminate was not reinforced along the through-thickness direction, E_3 was calculated using the rule of mixtures for transverse property [45]: $E_3 = \frac{E_m E_{f,t}}{v_f E_m + (1-v_f) E_{f,t}}$. Here, v_f is the fiber volume fraction and E_m and $E_{f,t}$ are the Young's modulus of the matrix and the fiber along the transverse directions, respectively. The values of $v_f = 50\%$, $E_m = 2750$ MPa, $E_{f,t}$ (E-glass) = 72000 MPa were used to estimate the E_3. The shear modulus in three planes was obtained using the following relations [45,46]: $G_{12} = \frac{1}{\frac{4}{E_x} - \frac{1}{E_1} - \frac{1}{E_2} + \frac{2\vartheta_{12}}{E_1}}$, $G_{13} = G_{23} = \frac{E_3}{2(1+\vartheta_{13})}$.

Table 3. Specifications of the used materials.

Material	E_1 (GPa)	E_2 (GPa)	E_3 (GPa)	υ_{12}	υ_{13}	υ_{23}	G_{12} (GPa)	G_{13} (GPa)	G_{23} (GPa)
Epoxy/glass fiber composite	9890	9890	5300	0.13	0.41	0.41	1580	1880	1880
Cork	5.10	5.10	5.10	0.10	0.10	0.10	5.90	5.90	5.90
PU foam	7.22	7.22	7.22	0.21	0.05	0.05	0.05	2.98	2.98

According to the literature survey, the Poisson's ratios: υ_{12} and $\upsilon_{13} = \upsilon_{23}$ for woven glass fiber reinforced composites are in the range of about 0.13-0.18 and 0.38-0.41, respectively [45-47]. In this study, υ_{12} and $\upsilon_{13} = \upsilon_{23}$ assumed to be equal to 0.13, and 0.41 [45].

Other material parameters such as Poisson's ratios of cork and PU foam, that were not determined experimentally, were obtained from manufacturer's data and published literature [15,38,48,49].

This is the accepted manuscript (postprint) of the following article:
Najafi, M., & Eslami-Farsani, R. (2021). Design and characterization of a multilayered hybrid cored-sandwich panel stiffened by thin-walled lattice structure. *Thin-Walled Structures*, *161*, 107514.
https://doi.org/10.1016/j.tws.2021.107514

4.1.2. Water absorption behavior

Fig. 10 illustrates the variation of weight uptake for PU, PU/S, and PU/C/S specimens as a function of the immersion days in freshwater. Visual examination of the specimens indicated some dimensional changes in the PU and PU/S specimens following 100 days of exposure to the wet environmental conditioning.

It was observed from Fig. 10 that the maximum weight uptake of PU specimen after 100 days of immersion in freshwater reached a significant value of 486.21%. While, it can be clearly observed that the maximum weight uptake for PU/S and PU/C/S specimens was much lower than the PU specimens, during the same period of environmental conditioning (i.e. 100 days).

Although the initial weigh uptake rates were similar for PU/S and PU/C/S specimens, the differences were gradually apparent after about 10 days, and the final weight uptake of PU/S and PU/C/S specimens was found to be 121.42% and 57.98%, respectively. As expected, the presence of thin layers of cork could reduce the water uptake of the PU/C/S specimens by more than 50% in comparison to those of PU/S. Despite the relatively low fraction volume of the cork in the structure of PU/C/S specimens, i.e. only 20%, the excellent barrier performance of this natural material could successfully prevent the water ingress from the upper and lower faces of the hybrid specimen. Nevertheless, the level of weight uptake in PU/C/S specimens was expected to be even much lower than the reported value. Therefore, the weight uptake in PU/C/S specimens was most likely contributed by the PU foam part since several studies reported that the gas and fluid permeability in cork products is usually negligible [36,50,51]. The intrinsic porosity on the PU foam surface as well as insufficient sealing of the open edges of the target specimens were probably responsible for the remarkable ingress of water into the hybrid specimens (i.e. PU/C/S). Therefore, the lower absorption level is to be expected in a

This is the accepted manuscript (postprint) of the following article:
Najafi, M., & Eslami-Farsani, R. (2021). Design and characterization of a multilayered hybrid cored-sandwich panel stiffened by thin-walled lattice structure. *Thin-Walled Structures*, *161*, 107514.
https://doi.org/10.1016/j.tws.2021.107514

real case, where only the upper or lower surfaces of the marine panel are exposed to environmental conditions, and the free edges of the panel are usually not in contact with the wet environment.

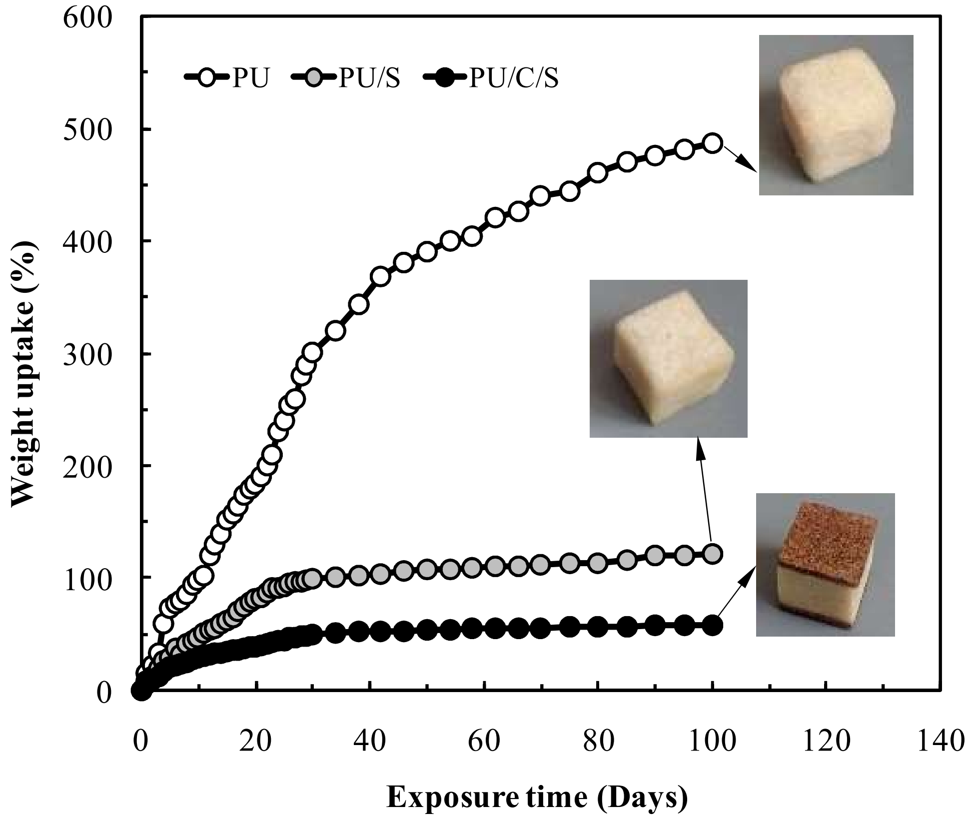

Fig. 10. Weight uptake in PU, PU/S, and PU/C/S specimens immersed in freshwater vs. exposure time.

4.2. Sandwich panels characterization

4.2.1. Flexural properties

Fig. 11 depicts the typical load-displacement curves of the 3 PB tests for two sandwich systems which were selected based on the closest curves to average values. As can be observed from this figure, the flexural behavior of two specimen types (i. e. SP1 and SP2) can be categorized into three major stages:

This is the accepted manuscript (postprint) of the following article:
Najafi, M., & Eslami-Farsani, R. (2021). Design and characterization of a multilayered hybrid cored-sandwich panel stiffened by thin-walled lattice structure. *Thin-Walled Structures*, *161*, 107514.
https://doi.org/10.1016/j.tws.2021.107514

(I) In the first stage of testing, both specimen types exhibited an elastic-linear response without any visual damage up to the second stage. The initial flexural stiffness was easily evaluated from the slope of the linear portion of load-displacement curves. As can be seen from the presented curves, the conceptual structural changes in SP2 systems could successfully enhance the flexural performance of studied sandwich panels.

(II) The second stage began with deviation from linear behavior which was mainly accompanied by a local deformation in the PU foam, followed by the reduction of curve slope until the maximum flexural load. The results clearly showed that the nonlinear behavior of SP1 is much higher than that of SP2 specimens. The considerable stiffness softening and nonlinear behavior in SP1 specimens can be attributed to the crushable nature of PU foam. While, in SP2 specimens, this PU behavior has been affected by the composite lattice structure, providing a uniform stiffness at the regular intervals and eliminating the extensive deformations as well as dominant nonlinear behavior until the maximum flexural load value is reached.

(III) In the third stage, the core-composite components debonding and core densification were accompanied by a reduction in the applied load which was gradually continued until the ultimate failure of the specimens. Due to the multiplicity of structural components in SP2 specimens, various types of structural failure mechanisms were observed at this stage. The fluctuation of the load displacement curve clearly indicates the progressive failure mechanisms and load-bearing capacity of integrated structural components in SP2 specimens.

This is the accepted manuscript (postprint) of the following article:
Najafi, M., & Eslami-Farsani, R. (2021). Design and characterization of a multilayered hybrid cored-sandwich panel stiffened by thin-walled lattice structure. *Thin-Walled Structures*, *161*, 107514.
https://doi.org/10.1016/j.tws.2021.107514

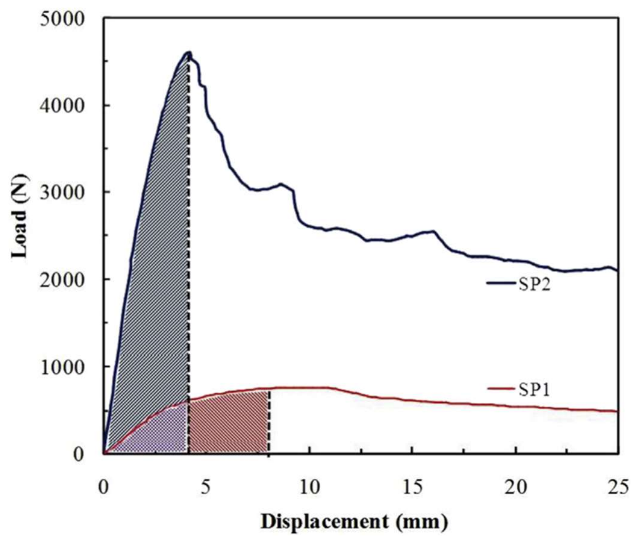

Fig. 11. Load-displacement curves for SP1 and SP2 specimens under the 3 PB test.

To make a better comparison, the flexural values obtained from the load-displacement curves are summarized in Table 4. Accordingly, SP1 specimens demonstrated the initial flexural stiffness of 184 N/mm and the maximum flexural load of 759 N. Similarly, the initial flexural stiffness and the maximum flexural load of SP2 specimens were found to be 1685 N/mm and 4596 N, respectively. Thus, it can be concluded that the substituting the conventional PU foam cores with multilayered hybrid core stiffened by composite lattice structure has a remarkable increase of 506% and 816% in flexural load and initial flexural stiffness, respectively.

Table 4. 3PB test results for SP1 and SP2 sandwich systems.

Specification	SP1	SP2
Maximum flexural load (N)	759 ± 9	4596 ± 53
Specific maximum flexural load (N.m^2/Kg)	90.1	546.5
Initial flexural stiffness (N/mm)	184 ± 3	1685 ± 10
Specific initial flexural stiffness (kN.m/kg)	21.9	200.2
Deflection at maximum load (mm)	8.85 ± 1.3	4.19 ± 0.6
Area under the curve (N.mm)	4773 ± 93	11693 ± 344

The specific mechanical properties which are defined by measured properties/weight ratio are always one of the key aspects for structural designers, especially in the field of lightweight structures such as composite vessels. Since the areal weight of the two sandwich systems is almost equal (8-41-8.42 kg/m^2), the specific flexural values of SP2 specimens have increased by the same proportions as previously mentioned.

The total area under the flexural load-displacement curve can be somehow as a representative of the flexural toughness in sandwich specimens [36]. The value of the area under the curve up to the maximum load point for SP1 and SP2 specimens which is assigned by the hatch pattern shown in Fig. 11 is 4773 N mm and 11693 N mm, respectively. These results can guarantee the higher energy absorption capability of the SP2 specimens compared to SP1 specimens.

The high structural stiffness of SP2 compared to SP1 specimens could dramatically reduce the deflection at the point of maximum flexural load. As can be seen from Fig. 11 and Table 4, the vertical deflection at the maximum flexural load for SP1 and SP2 specimens measured 8.85 and 4.19 mm, respectively.

To better understand the nature of the failure modes and their dependence on the structural response of the two different types of sandwich systems, the photographs of the specimens during and after the flexural testing were prepared. The 3 PB testing sequences of SP1, as well as the ultimate failure modes in this specimen, are depicted in Figs. 12 and 13, respectively.

This is the accepted manuscript (postprint) of the following article:
Najafi, M., & Eslami-Farsani, R. (2021). Design and characterization of a multilayered hybrid cored-sandwich panel stiffened by thin-walled lattice structure. *Thin-Walled Structures*, *161*, 107514.
https://doi.org/10.1016/j.tws.2021.107514

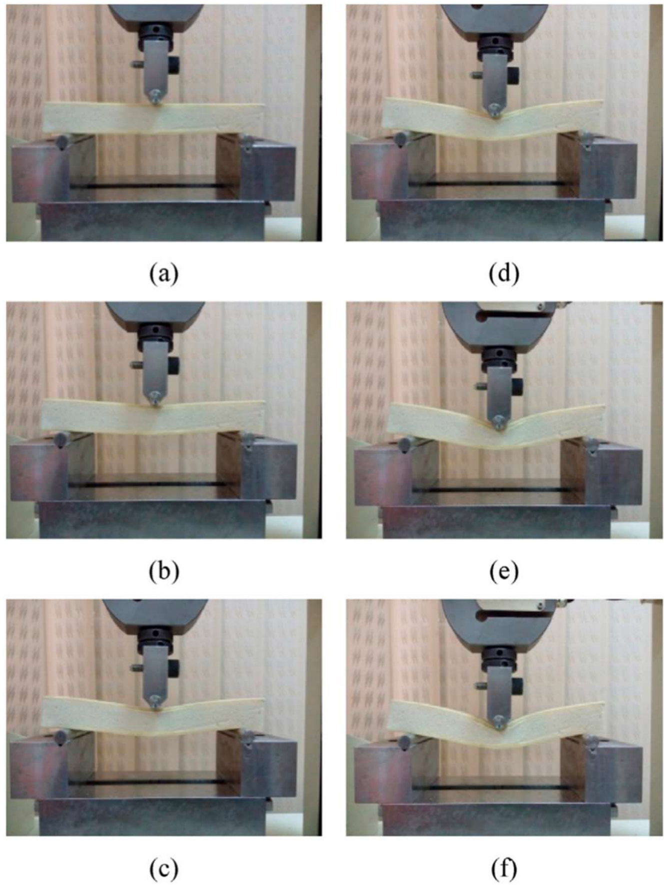

Fig. 12. Sequence of 3 PB test performed on SP1 specimen at displacement of (a) 0 mm, (b) 5 mm, (c) 10 mm, (d) 15 mm, (e) 20 mm, (f) 25 mm.

This is the accepted manuscript (postprint) of the following article:
Najafi, M., & Eslami-Farsani, R. (2021). Design and characterization of a multilayered hybrid cored-sandwich panel stiffened by thin-walled lattice structure. *Thin-Walled Structures*, *161*, 107514.
https://doi.org/10.1016/j.tws.2021.107514

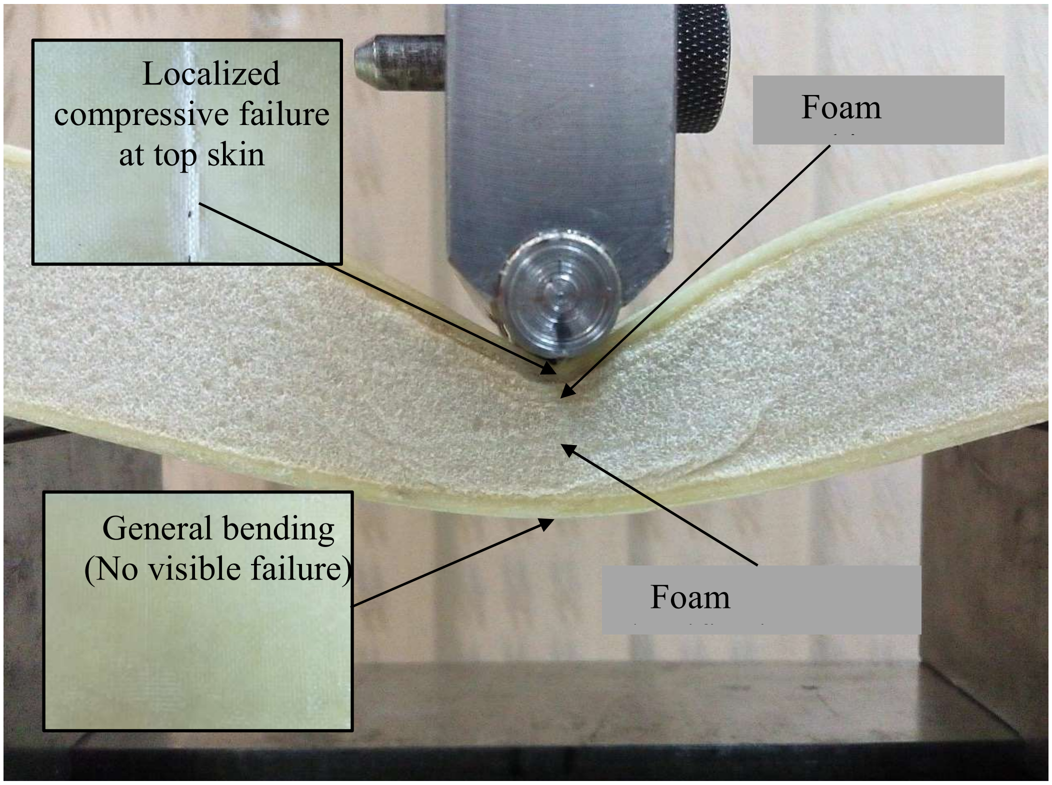

Fig. 13. Failure modes in SP1 specimen under the 3PB test.

As can be seen from the photographs presented in Fig. 12, SP1 specimens exhibited a general bending behavior along the beam length up to the deflection of about 10 mm, followed by a gradual local deformation beneath the loading head. Meanwhile, the top skin suffered a local compressive failure in the vicinity of the loading point. The extent and depth of the mentioned failure were intensified with increasing the load. A thorough examination revealed that no visible damage was occurred in the bottom skin, indicating its low contribution in loadbearing compared to the top skin.

The localized compressive deformation of the structure, extensive foam densification, and foam crushing in a symmetrical pattern as the ultimate failure modes in SP1 specimen can be observed in Fig. 13.

This is the accepted manuscript (postprint) of the following article:
Najafi, M., & Eslami-Farsani, R. (2021). Design and characterization of a multilayered hybrid cored-sandwich panel stiffened by thin-walled lattice structure. *Thin-Walled Structures*, *161*, 107514.
https://doi.org/10.1016/j.tws.2021.107514

Similarly, in Figs. 14 and 15, the progressive failure development under 3 PB testing and the final failure modes for the SP2 specimens are shown. By carefully examining the sequences of specimen loading in Fig. 14, it could be concluded that the general bending behavior in SP2 specimens was clearly lower than those of SP1. The change in the form of the local deformation from open U-shaped to V-shaped (Figs. 12 and 14) is quite obvious which indicates a different structural response of the two sandwich systems against bending load.

The localized compressive failure in top skin was occurred at a relatively slight deformation (less than 5 mm), followed by gradual buckling of the transverse central, as the loading process continued stiffener (Fig. 14(c) and (d)). In this case, two longitudinal stiffeners along the length of the beam tolerated large amounts of load and dramatically increase the load-bearing capacity of the structure. The local indentation as the dominant failure mode is observable in longitudinal stiffeners.

This is the accepted manuscript (postprint) of the following article:
Najafi, M., & Eslami-Farsani, R. (2021). Design and characterization of a multilayered hybrid cored-sandwich panel stiffened by thin-walled lattice structure. *Thin-Walled Structures*, *161*, 107514.
https://doi.org/10.1016/j.tws.2021.107514

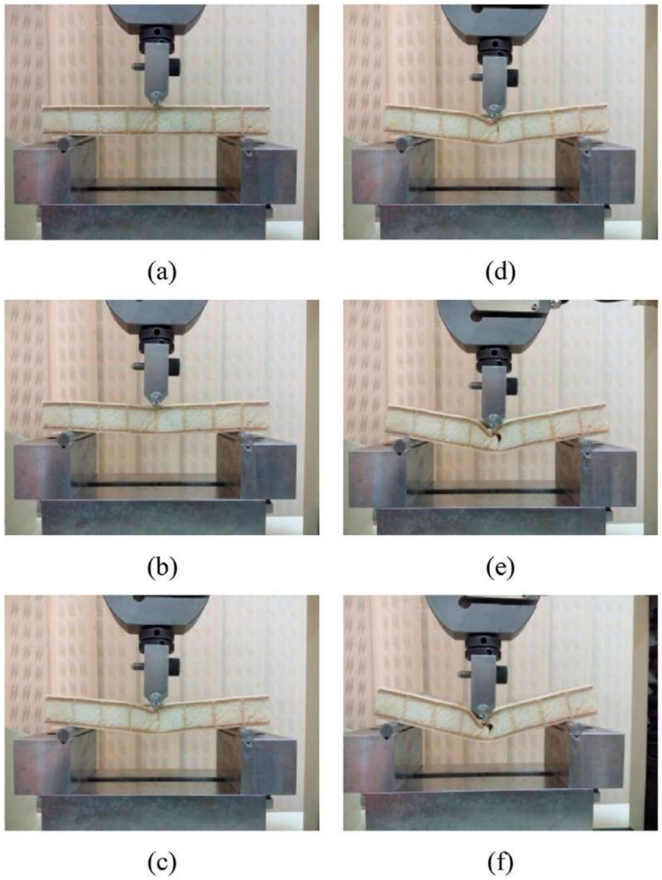

Fig. 14. Sequence of 3 PB test performed on SP2 specimen at displacement of (a) 0 mm, (b) 5 mm, (c) 10 mm, (d) 15 mm, (e) 20 mm, (f) 25 mm.

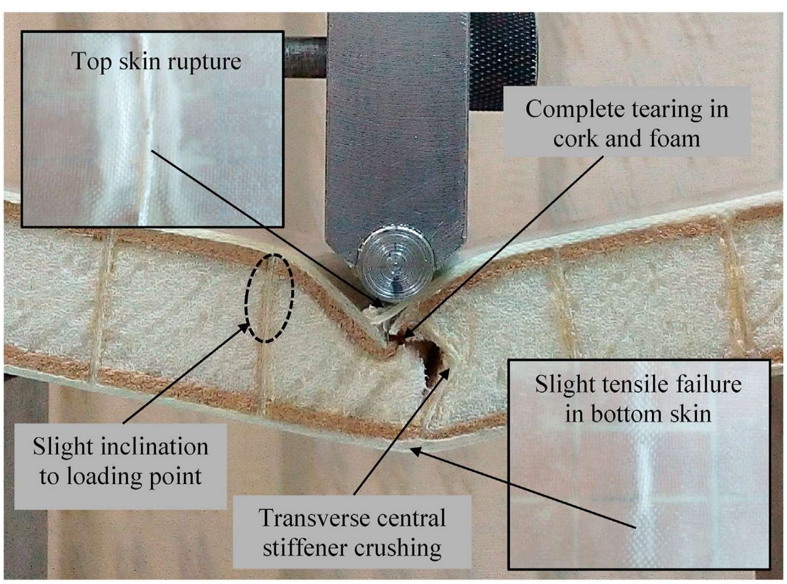

Fig. 15. Failure modes in SP2 specimen under the 3 PB test.

In the final stages of loading, transverse stiffeners adjacent to the midspan of the specimen were slightly inclined to the loading region which implies their active contribution in withstanding a significant portion of the applied load. It can be clearly observed that the transverse central stiffener was crushed, and top skin, as well as agglomerated cork and PU foam, were completely failed at the contact location between loading head and skin (Fig. 15). Several white cracks along the stiffeners/skin bonding lines indicate the local resin cracking in the bottom skin. Despite the inconsistency of the agglomerated cork and PU foam, it was evident that their bonding was well established even in the final stages of loading. It can be attributed to the instincts roughness of cork's external surface, providing the appropriate conditions for better mechanical interlocking of adjacent materials.

The presence of minor damages in the bottom skin indicates the appropriate contribution of all structural components in the load-bearing process. As can be seen from Fig. 15, both the longitudinal and transverse stiffeners remain well attached to the top and bottom skins which may indicate the adequate quality of manufactured specimens.

From the observations, utilization of a thin-walled lattice structure has led to the improved load-bearing capacity of the structure in different ways, as follows:

(I) Increasing of bonding strength between the core and skin, resulting in an enhancement of delamination resistance of the structure;

(II) Increasing compressive stiffness and strength of core in through thickness direction;

(III) Restricting the large deformations in foam which prevented the foam from general and extensive crushing;

(IV) Providing more structural integrity by connecting the top and bottom skins, resulting in more uniform stress distribution and better stress transfer across the structure.

This is the accepted manuscript (postprint) of the following article:
Najafi, M., & Eslami-Farsani, R. (2021). Design and characterization of a multilayered hybrid cored-sandwich panel stiffened by thin-walled lattice structure. *Thin-Walled Structures*, *161*, 107514.
https://doi.org/10.1016/j.tws.2021.107514

4.2.2. Flatwise compressive properties

The typical compressive load-displacement curves of the specimens are plotted in Fig. 16, which shows the compressive load-bearing capacity of the SP2 in comparison with the SP1 sandwich system. It can be seen that the load-displacement curve of SP1 specimen followed the typical behavior of cellular materials such as PU foam (without composite skin) [52], and its compression performance is only controlled by the core properties [53]. At the beginning of the test, the imperfect contact between the loading head/supports and specimens appeared as an initial load settlement in load-displacement curves. The SP1 specimen then exhibited a nearly linear elastic behavior till the peak load (maximum compressive load), followed by the large plateau region associated with the crushing of the foam's cell walls. Finally, the load increased with a steep slope due to the densification of the PU foam core which was accompanied by a higher compressive strength [29].

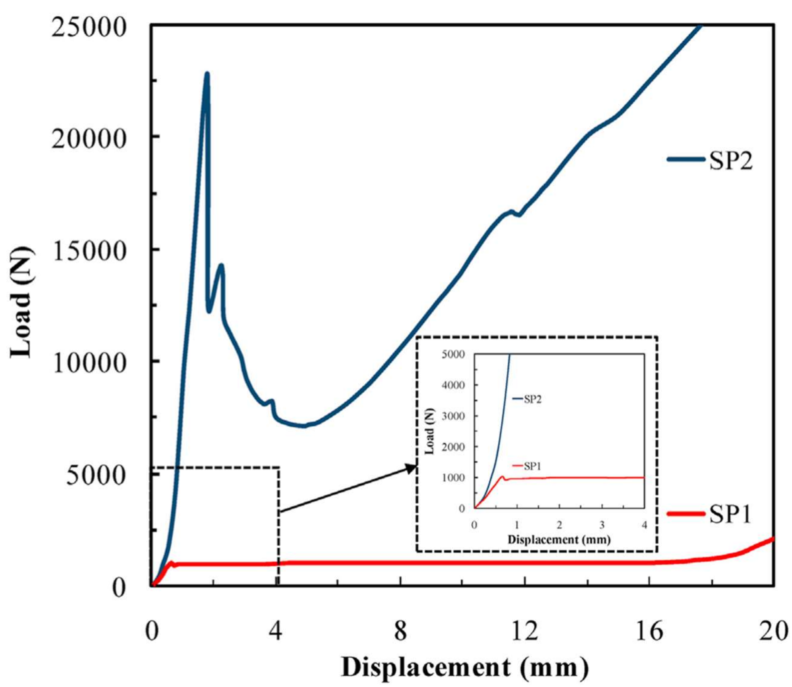

Fig. 16. Load-displacement curves for SP1 and SP2 specimens under the flatwise compression test.

This is the accepted manuscript (postprint) of the following article:
Najafi, M., & Eslami-Farsani, R. (2021). Design and characterization of a multilayered hybrid cored-sandwich panel stiffened by thin-walled lattice structure. *Thin-Walled Structures*, *161*, 107514.
https://doi.org/10.1016/j.tws.2021.107514

The typical failure modes of specimens under flatwise compression tests are illustrated in Fig. 17. As shown in Fig. 17 (a), foam densification was the prominent failure mode in SP1 specimens which is very similar to the pure PU foam subjected to this type of compressive loading.

For the lattice sandwich panels with a multilayered hybrid core, SP2 specimens exhibited a linear-elastic response up to the maximum compressive load in the first stage. During the test, the composite lattice structure successfully carried most of the applied load which was followed by the occurrence of buckling in lattice stiffeners. Thus, the second stage of deformation was accompanied by a sudden drop in load capacity of the structure. After this point, by reducing the load-bearing capacity of the lattice structure, the foam densification consequently occurred and load increased again as reported in previous studies [38,54].

(a)

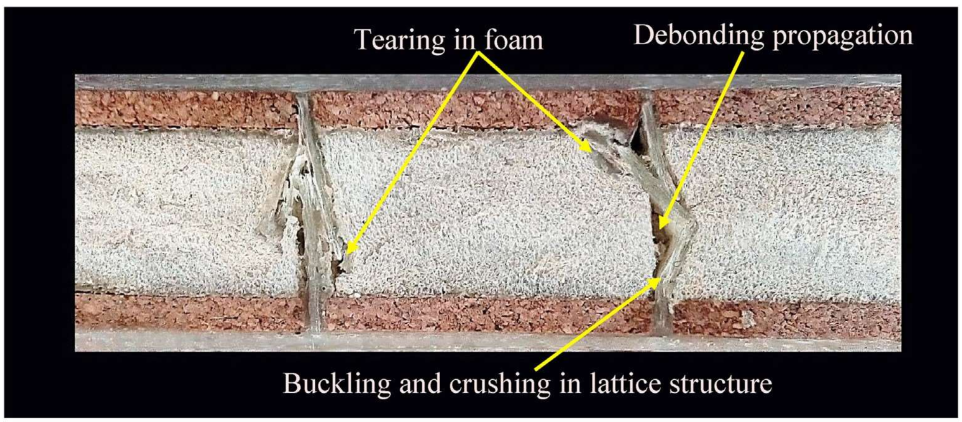

(b)

Fig. 17. Failure modes in (a) SP1, (b) SP2 specimens, under flatwise compression test.

For a more detailed examination of the failure modes in SP2 specimens, the specimen's surrounding edges were mechanically cleaned. It was seen that the composite stiffeners were completely buckled and the debonding propagated near the stiffener/core region. The sharp pieces branched from the broken stiffeners were also observed to be violently scraped and penetrated into PU foam, as shown in Fig. 17 (b).

The results of the flatwise compression tests for SP1 and SP2 are summarized in Table 5. Accordingly, the maximum compressive load and compressive stiffness for SP1 specimens were found to be an average value of 1044 N and 1343 N/mm, respectively. By comparing the compressive properties of the control specimen (SP1) and novel system (SP2), the remarkable effect of proposed modifications can be clearly observed where without increasing the structural weight, the maximum compressive load of the SP2 specimens has exceptionally increased to about 2080% over the SP1 specimens.

Table 5. Flatwise compression test results for SP1 and SP2 sandwich systems.

Specification	SP1	SP2
Maximum compressive load (N)	1044 ± 4	22754 ± 259
Specific maximum compressive load (N.m^2/Kg)	124.0	2705.6
Compressive stiffness (N/mm)	2343± 5	17899 ± 101
Specific compressive stiffness (kN.m/kg)	159.7	2128.3
Deflection at maximum load (mm)	0.62 ± 0.1	1.77 ± 0.3

The initial compressive stiffness of SP2 specimens had an average value of 17899 N/mm, which was more than 12 times higher than that of the SP1. Unlike the flexural results, it can also be observed that the deflection at the maximum load of SP2 specimens was higher than that of SP2. The average of the deflection at maximum load recorded for SP1 and SP2 specimens was 0.62 mm and 1.77 mm, respectively.

4.2.3. Edgewise compressive properties

The typical load-displacement curves and failure modes of studied sandwich panels under edgewise compression tests are displayed in Figs. 18 and 19, respectively. For SP1, before the maximum compressive load, the specimen exhibited a nearly linear elastic behavior with no significant failure (Fig. 18).

As shown in Fig. 19 (a), when the load reached its maximum value, the global buckling in the specimen was starting to happen, followed by the progressive local failure of composite skins in the middle of the specimen. The PU foam was then densified inwardly in a symmetric and triangular pattern around the axis of damage formed on the sandwich skin. It should be noted that a considerable amount of deformation in the foam was not recovered even after unloading and therefore was remained permanently in SP1 specimens.

Similarly, for SP2 specimens, no significant failure was observed before reaching the initial peak of the load-displacement curve which was accompanied by the linear elastic response similar to the observations made in SP1 specimens (Fig. 18). After the initial peak, the load abruptly decreased due to the shearing slip damage and wrinkling of composite skins close to the lower part of the specimen, as shown in Fig. 19 (b). As it is evident in 19 (b), the broken pieces of skin effectively behaved as the end supports of the lower lattice stiffener against the direction of loading, allowing the load to increase again. Following that, the load gradually increased in a zigzag pattern (Fig. 18), until the lower lattice stiffener was completely bent (Fig. 19 (b)) and the load dropped again, as shown in Fig. 18. As seen in Fig. 19 (b), the SP2 specimens also suffered from the shear cracks in both the cork and PU foam at the final stage of compressive testing.

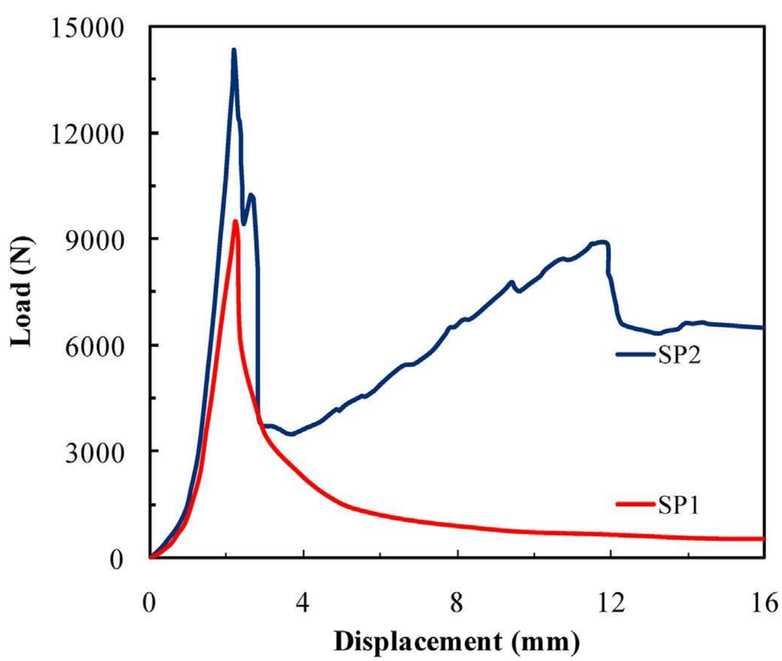

Fig. 18. Load-displacement curves for SP1 and SP2 specimens under the edgewise compression test.

This is the accepted manuscript (postprint) of the following article:
Najafi, M., & Eslami-Farsani, R. (2021). Design and characterization of a multilayered hybrid cored-sandwich panel stiffened by thin-walled lattice structure. *Thin-Walled Structures*, *161*, 107514.
https://doi.org/10.1016/j.tws.2021.107514

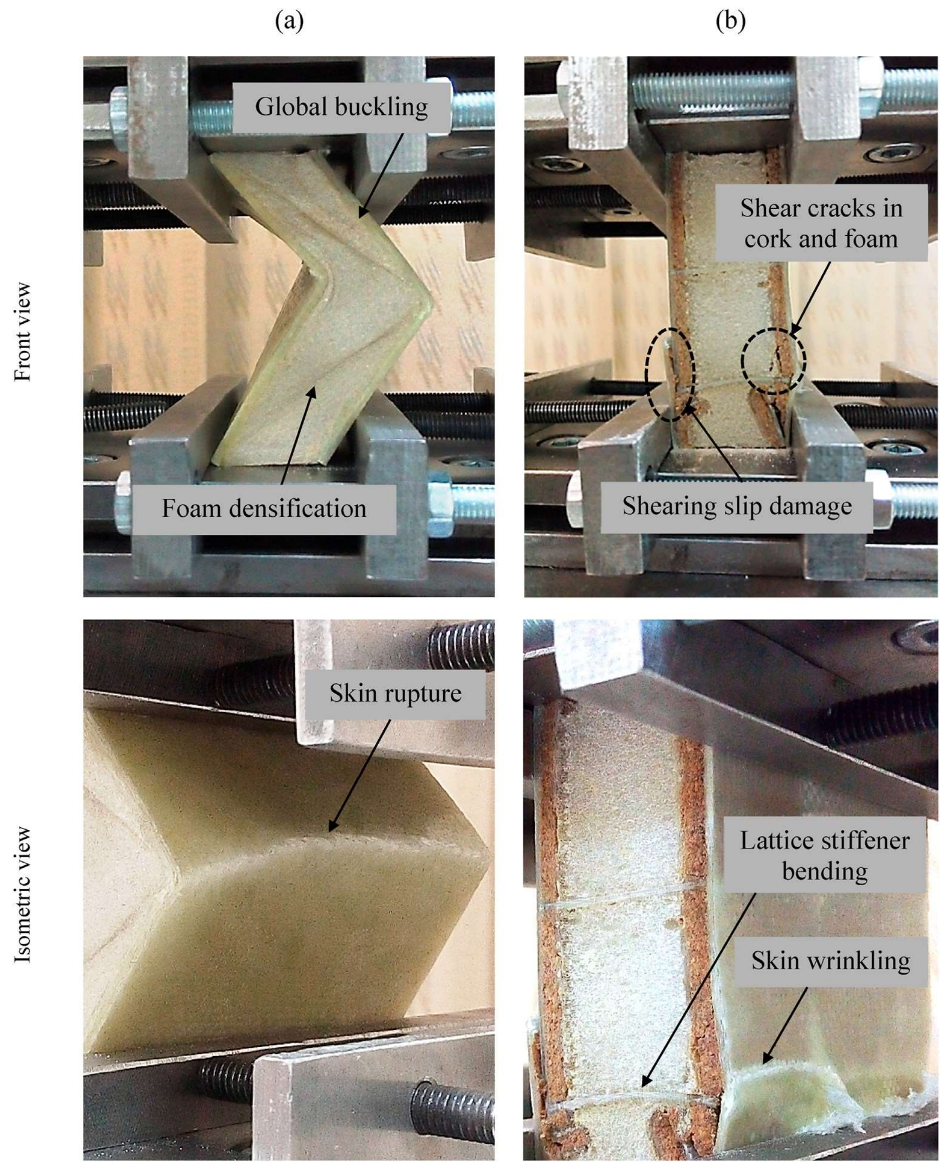

Fig. 19. Failure modes in (a) SP1, (b) SP2 specimens, under the edgewise compression test.

Table 6 summarize the average compressive properties of sandwich specimens in edgewise mode. Accordingly, the maximum compressive load and compressive stiffness values obtained from edgewise compressive testing for the SP1 specimens were 9729 N and 8260 N/mm, respectively. Similarly, the maximum compressive load and compressive stiffness of SP2 specimens were found to be 14273 N and 8904 N/mm, respectively. It can be concluded from the results that the maximum compressive load and compressive stiffness values were about 47% and 8%, respectively, higher than those offered by the SP1 specimens. Needless to say, the edgewise compressive properties of PU foam-cored sandwich panels were not significantly affected by the proposed structural modifications. These results can be attributed to the inherent structural response of sandwich panels to loading type, where unlike the flatwise compression, both the core and skins contribute in the loadbearing process and therefore, the differences between the test results of two sandwich systems were remarkably smaller than those of flatwise compression. Finally, the deflection at maximum load of SP1 and SP2 specimens were 2.44 mm and 2.35 mm, respectively, which is close enough that no further consideration is required.

Table 6. Edgewise compression test results for SP1 and SP2 sandwich systems.

Specification	SP1	SP2
Maximum compressive load (N)	9729 ± 159	14273 ± 44
Specific maximum compressive load (N.m^2/Kg)	1155.5	1697.1
Compressive stiffness (N/mm)	8260 ± 131	8904 ± 26
Specific compressive stiffness (kN.m/kg)	981.0	1058.7
Deflection at maximum load (mm)	2.44 ± 0.3	2.36 ± 0.2

4.2.4. Quasi-static indentation behavior

The indentation load versus displacement for SP1 and SP2 specimens are shown in Fig. 20. As the test began, the load increased almost linearly with the displacement, until the load reached the yield point (maximum indentation load). The load level then decreased slightly and it remained almost constant until about 9-10 mm. As usual in previous tests, the foam densification then occurred, followed by the complete crushing of foam and localized failure in top skin which simultaneously led to a re-increase of the load in the load-displacement curve. The test immediately ended with complete perforation in the bottom skin.

This is the accepted manuscript (postprint) of the following article:
Najafi, M., & Eslami-Farsani, R. (2021). Design and characterization of a multilayered hybrid cored-sandwich panel stiffened by thin-walled lattice structure. *Thin-Walled Structures*, *161*, 107514.
https://doi.org/10.1016/j.tws.2021.107514

Comparing the load-displacement curves of two specimens, it was clearly observed that the use of the thin-walled lattice structure has a tremendous effect on improving the indentation resistance of PU foam-cored sandwich panels. It was concluded that the cross-stiffener played as a strong column at the center of the specimen and could successfully resist the concentrated indentation load during the whole testing process.

As can be seen from Fig. 20, the load-displacement curve of SP2 specimen was relatively similar to that seen in the flexural properties. The SP2 specimen exhibited a nearly linear response up to the maximum load level, followed by various fluctuations in the load-displacement curve which can be attributed to a sequential failure in top skin and lattice structure. After the displacement reached a value equal to that of the control specimen (SP1), the test was intentionally stopped for making the comparative investigations. Here, no significant densification occurred in the foam and the indenter could not even reach the bottom skin.

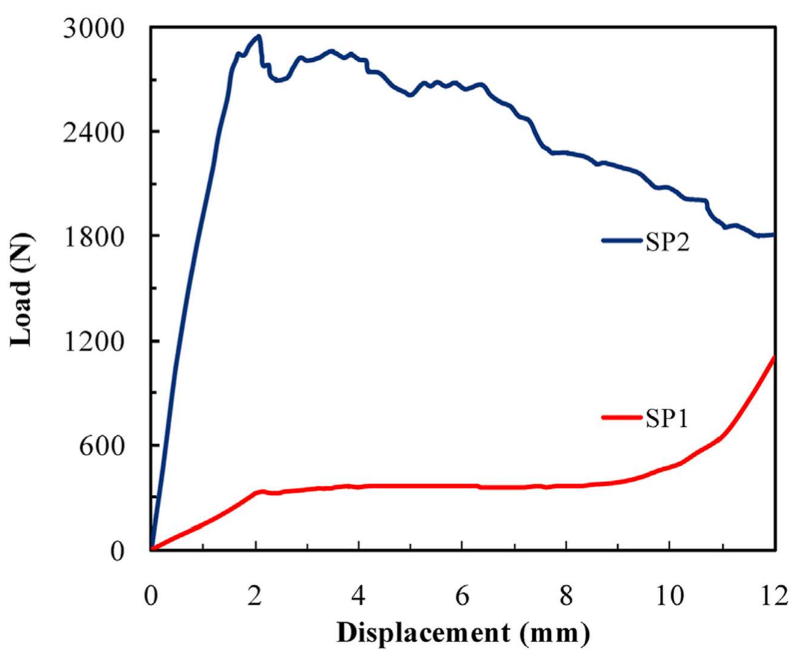

Fig. 20. Load-displacement curves for SP1 and SP2 specimens under concentrated quasi-static indentation test.

The results of concentrated quasi-static indentation tests are given in Table 7. As can be seen from the table, The SP1 specimens showed the average maximum indentation load of 328 N and the average indentation stiffness of 158 N/mm. In the same way, the average maximum indentation load and indentation stiffness of SP2 specimens were found to be 2933 N and 2171 N/mm, respectively. Therefore, the synergistic effect of flexible cork layers and stiff composite lattice stiffeners within the structure of these novel sandwich panels resulted in a dramatic increase of about 794% in maximum indentation load and 1274% in indentation stiffness compared to the traditional PU foam-cored sandwich panels (i.e. SP1).

Table 7. Concentrated quasi-static indentation test results for SP1 and SP2 sandwich systems.

Specification	SP1	SP2
Maximum indentation load (N)	328 ± 15	2933 ± 102
Specific maximum indentation load (N.m^2/Kg)	39.0	348.8
Indentation stiffness (N/mm)	158 ± 13	2171 ± 94
Specific indentation stiffness (kN.m/kg)	18.8	258.1
Specific absorbed energy (kJ/kg)	6.2 ± 0.5	75.9 ± 5.1

Here, the capability of a structure to absorb the energy was defined as the specific absorbed energy (SAE) [55], which was the ratio of absorbed energy under the load-displacement curve up to the maximum load point per unit of specimen mass. The SAE level was calculated as 75.9 kJ/kg for SP2 specimens which was approximately 12 times greater than that of the SP1 specimens (i. e. 6.2 kJ/kg). Fig. 21 depicts the energy-displacement curve of two sandwich systems under the concentrated quasi-static indentation loading, in which each energy value was separately determined by integrating the area under the load-displacement curve at a certain displacement. The excellent energy absorption behavior of SP2 specimens compared to

SP1, not only up to the maximum load point but also until the end of indentation loading, indicates maintaining the structural integrity of the panel during the whole testing process.

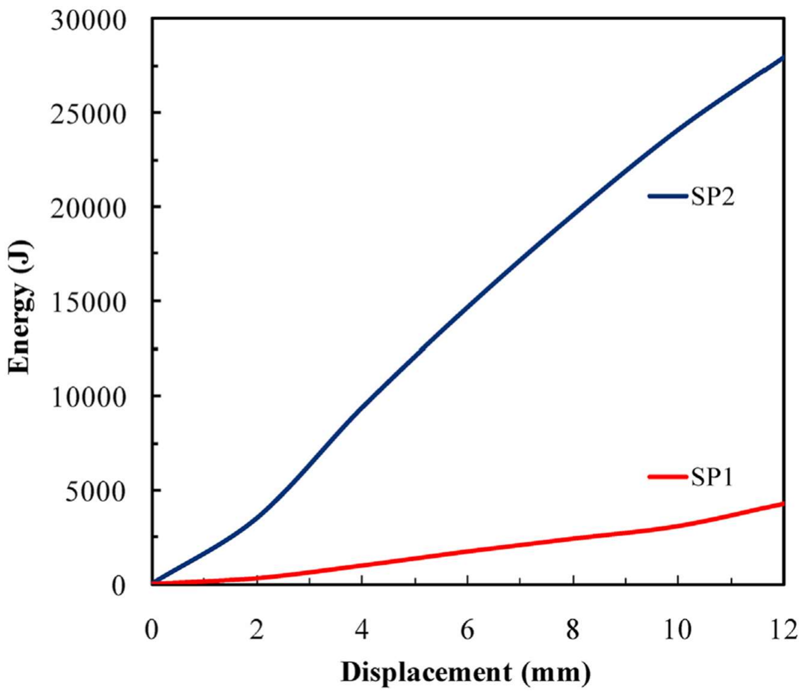

Fig. 21. Energy-displacement curves for SP1 and SP2 specimens under concentrated quasi-static indentation test.

Fig. 22 illustrates the front and rear views of two specimens subjected to quasi-static indentation loading. As can be seen from Fig. 22 (a), the top skin of the SP1 specimen showed a relatively symmetrical damage pattern in the form of a four-pointed star consisted of extensive delamination, fiber breakage, and fiber pull-out as the prominent damage mechanisms. A similar pattern of failure in the form of a small diamond was evident around the hole created in the top skin of the SP2 specimen, which represents the delamination at a limited level (Fig. 22 (b)). Due to the transparency of composite skins, a wide circular area representing the delamination and matrix cracking was clearly visible in the bottom skin of the SP1 specimen. The examination of bottom skin also indicated that the indenter could completely penetrate through the PU foam and made four shear petals on composite skin in a pyramid shape. In contrast to SP1, no traces of fiber breakage and indenter penetration into the bottom skin were visibly found in SP2 specimen and only small amounts of delamination and matrix cracking were observed in several areas, as shown in Fig. 22 (b).

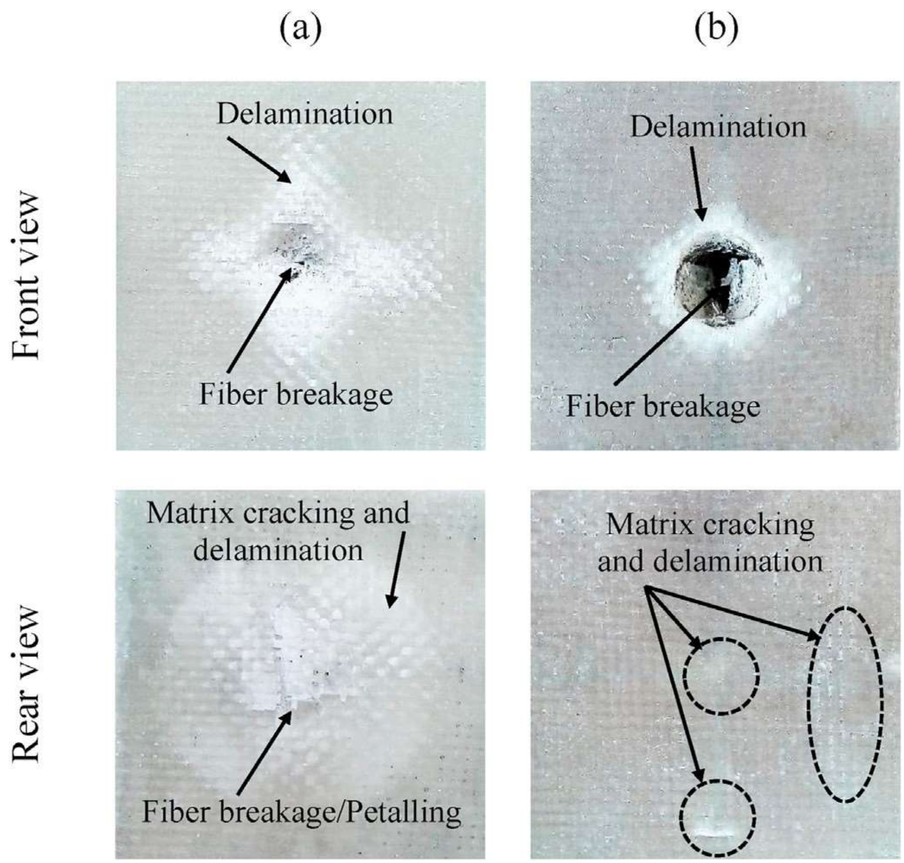

Fig. 22. Failure modes in (a) SP1, (b) SP2 specimens, under concentrated quasistatic indentation test.

4.2.5. High-velocity impact perforation behavior

Table 8 summarizes the high-velocity impact perforation test results including residual kinetic energy, absorbed impact energy, percentage of absorbed impact energy, and specific absorbed impact energy (normalized absorbed impact energy value by the areal density of the specimen). Accordingly, the absorbed impact energy of the SP2 specimens was found to be 225.62 J, which is approximately 21% greater than that offered by the SP1 specimens, i.e.

average value of 186.69 J. This means that the SP2 systems could successfully absorb 100% of the incident energy of the projectile, whereas this value for SP1 systems was 82.75% corresponding to a residual impact velocity of 54 m/s.

These results indicate that the simultaneous incorporation of cork and thin-walled lattice structure within the structure of PU foam-cored sandwich panels provided a superior high-velocity impact perforation resistance in this type of structure. The high flexibility and energy absorption capability of agglomerated cork compared to many conventional types of synthetic foams can potentially make it an excellent candidate for crashworthiness and high-velocity impact protection purposes [56,57].

Table 8. High-velocity impact perforation test results for SP1 and SP2 sandwich systems.

Specification	SP1	SP2
Initial velocity (m/s)	130	130
Residual velocity (m/s)	54 ± 6	0
Initial kinetic energy (J)	225.62	225.62
Residual kinetic energy (J)	38.93 ± 7.5	0.00
Absorbed impact energy (J)	186.69 ± 9.1	225.62
Percentage of absorbed impact energy (%)	82.75 ± 4.0	100
Specific absorbed impact energy ($J.m^2/Kg$)	22.20	26.83

Fig. 23 shows post-impact resultant failure modes in the impacted and non-impacted skins of the sandwich specimens. The visual examination of the SP1 specimen indicated the projectile could fully perforate through the thickness of the structure. The circumferential delamination around the impact location of impacted skin as well as the crushing of the core along the perforation path were dominant failure modes in SP1 specimens, as shown in Fig. 23 (a). The non-impacted skin of the SP1 specimens suffered full tearing in composite plies around the perforation hole in the form of a diamond shape accompanied by four dominant petals that

This is the accepted manuscript (postprint) of the following article:
Najafi, M., & Eslami-Farsani, R. (2021). Design and characterization of a multilayered hybrid cored-sandwich panel stiffened by thin-walled lattice structure. *Thin-Walled Structures*, *161*, 107514.
https://doi.org/10.1016/j.tws.2021.107514

emerged outwards. The non-impacted skin of the SP1 specimens experienced extensive delamination which is significantly larger than the diameter of the projectile (Fig. 23 (a)). As can be seen in Fig. 23 (a), fiber pull-out, and matrix cracking in a scattered pattern were also seen within the specimens. From the figure, the impact-induced shear loads could create a longitudinal splitting failure spreading across the half-width of the specimen.

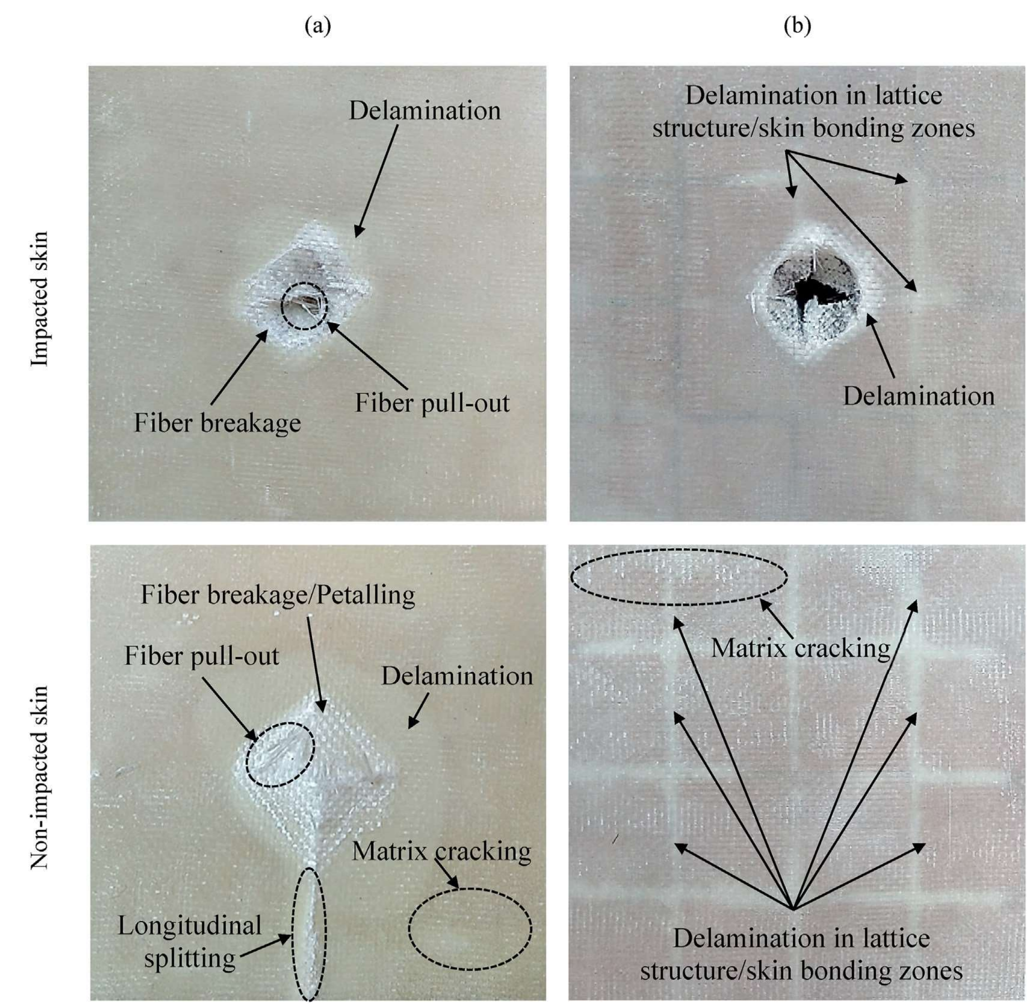

Fig. 23. Failure modes in (a) SP1, (b) SP2 specimens, subjected to high-velocity impact perforation test.

In the case of SP2 systems, the impacted skin exhibited a cylindrical penetration hole beneath the impact location associated with limited delamination around the circumferential edge of the indenter and cross-shaped delamination in several zones (Fig. 23 (b)). As expected, the projectile could not penetrate the non-impacted skin of SP2 specimens. The distributed matrix cracking and delamination in a regular grid pattern was clearly visible in all lattice stiffeners to skin bonding paths, as shown in Fig. 23 (b). This suggests that the localized impact load was uniformly distributed throughout the structure, and the lattice structure could fully contribute to the bearing of impact load which can be responsible for the outstanding response of SP2 panels under high velocity impact perforation loading. The extent of the zones affected by the delamination in non-impacted skins was clearly greater than those of impacted skins in both sandwich systems. This indicates a change of failure mode from local to general during the projectile penetration through the thickness of the structure. Furthermore, it is worth noting that no visible delamination was observed in lateral edges of SP2 specimens, indicating a proper interfacial bonding between agglomerated cork core and composite skins.

4.3. Numerical results

A series of numerical analysis was made to better understand the structural responses of two studied sandwich configurations. For this purpose, an applied load equal to the maximum load corresponding to each specimen type was conducted in accordance with the experimental results obtained from the three-point bending, edgewise compression, flatwise compression, and indentation tests.

Fig. 24 shows the comparison between load-displacement curves obtained from experimental and numerical results for SP1 and SP2 specimens. As can be seen in the figure, all numerical curves exhibited a nearly linear response until reaching the large displacements, which is attributed to the linear behavior of all structural constituents in the initial stages of loading. The nonlinear behavior for SP1 specimen under the bending load was evident, reflecting the elastic-plastic behavior of the PU foam core at higher displacements (i.e. after about 2 mm). It can be also observed that the displacement values associated with compression tests, especially in the edgewise mode were not matched well with experimental data. As mentioned earlier in experimental sections, the imperfect contact at loading points led to an initial load settlement in compressive load-displacement curves. The ideal conditions considered in the FE modeling completely eliminated this initial experimental error.

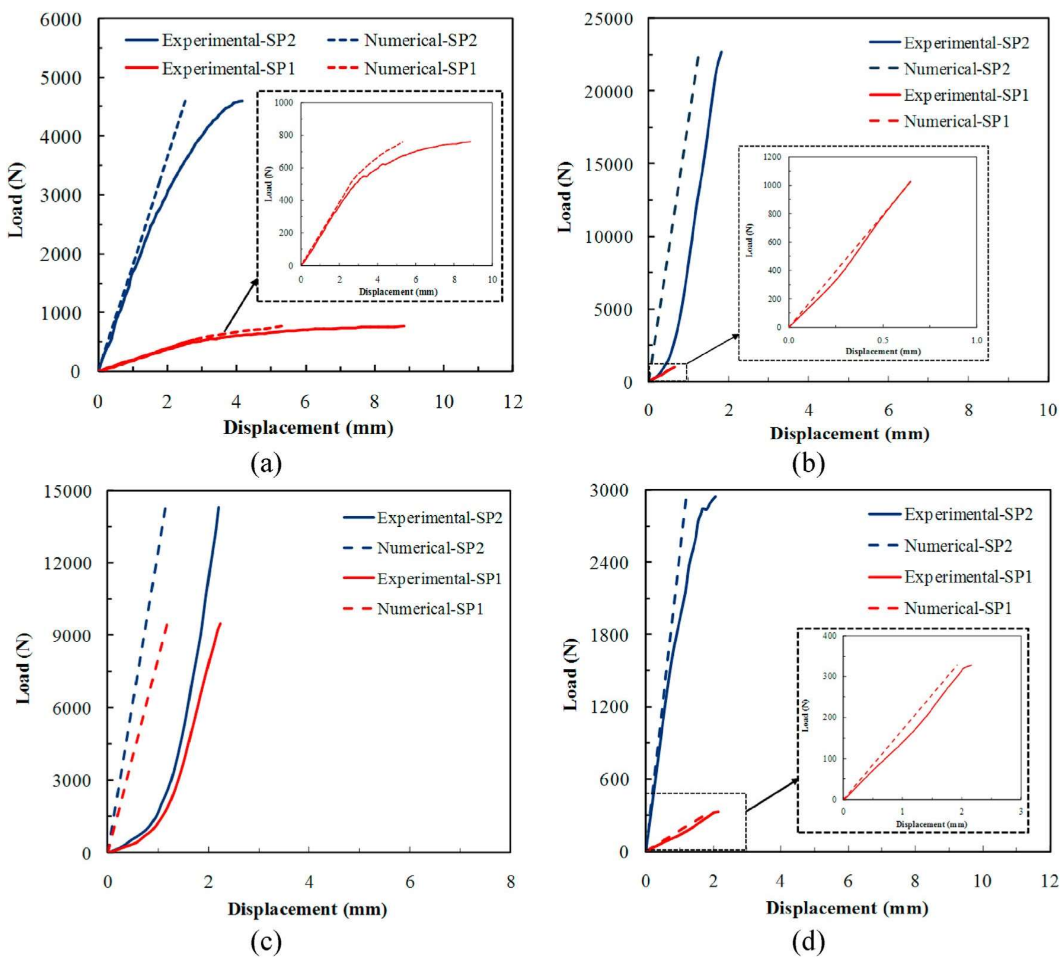

Fig. 24. Comparison between experimental and numerical results for SP1 and SP2 specimens under (a) 3 PB, (b) Flatwise compression, (c) Edgewise compression, (d) concentrated quasi-static indentation test.

The FE model predicted the initial flexural stiffness, compressive stiffness in flatwise mode, compressive stiffness in edgewise mode, and indentation stiffness of 1818, 18009, 12450, and 1450 N/mm for SP2 specimens, respectively, which were 837%, 1041%, 55%, and 1333%, respectively, more than those of SP1 specimens. These results suggest that the numerical model could reasonably estimate the stiffness of both sandwich systems in different loading conditions. The good agreement observed can be justified by the linear-elastic behavior of all structural constituents in the initial stages of loading which was closely matched with the mechanical properties assigned to the numerical models. On the other hand, the relatively small overestimation of stiffness can be attributed to the initial assumption in which the core-skin interface was considered to be perfectly bonded without any initial defect. In the following, as the load increased, a growing divergence between the numerical and experimental curves was observed. These observations are most likely attributed to some variables related to the manufacturing process, geometrical nonlinearity and asymmetry occurred during the experiments which were not taken into account in the FE model.

To provide a better comparison, numerical simulations were then conducted by applying the same load on two specimen types. Accordingly, the vertical loads of 500, 1000, 5000, and 300 N, respectively, were selected as the applied load to determine the structural response of two structural configurations in bending, flatwise compression, edgewise compression, and indentation loads, as shown in Table 9. It should be noted that a relatively good match was found between the experimental and numerical results in above-mentioned loading values. The distribution contours of deformation, equivalent stress in composite parts, and compressive stress in PU foam for SP1 and SP2 specimens is also illustrated in Fig. 25.

This is the accepted manuscript (postprint) of the following article:
Najafi, M., & Eslami-Farsani, R. (2021). Design and characterization of a multilayered hybrid cored-sandwich panel stiffened by thin-walled lattice structure. *Thin-Walled Structures*, *161*, 107514.
https://doi.org/10.1016/j.tws.2021.107514

Table 9. Numerical results for SP1 and SP2 sandwich systems under 3 PB, flatwise compression, edgewise compression, and concentrated quasi-static indentation loads.

Loading Type	Applied force (N)	Specimen Type	Maximum deflection (mm)	Equivalent stress in composite parts (MPa)	Compressive stress in PU foam (MPa)
Three-point bending	500	SP1	2.72	27	0.09
		SP2	0.28	23	0.01
Flatwise compression	1000	SP1	0.64	0.5	0.16
		SP2	0.05	15	0.01
Edgewise compression	5000	SP1	0.62	55	0.06
		SP2	0.40	32	0.08
Concentrated quasi-static indentation	300	SP1	1.76	80	0.15
		SP2	0.12	26	0.01

This is the accepted manuscript (postprint) of the following article:
Najafi, M., & Eslami-Farsani, R. (2021). Design and characterization of a multilayered hybrid cored-sandwich panel stiffened by thin-walled lattice structure. *Thin-Walled Structures*, *161*, 107514.
https://doi.org/10.1016/j.tws.2021.107514

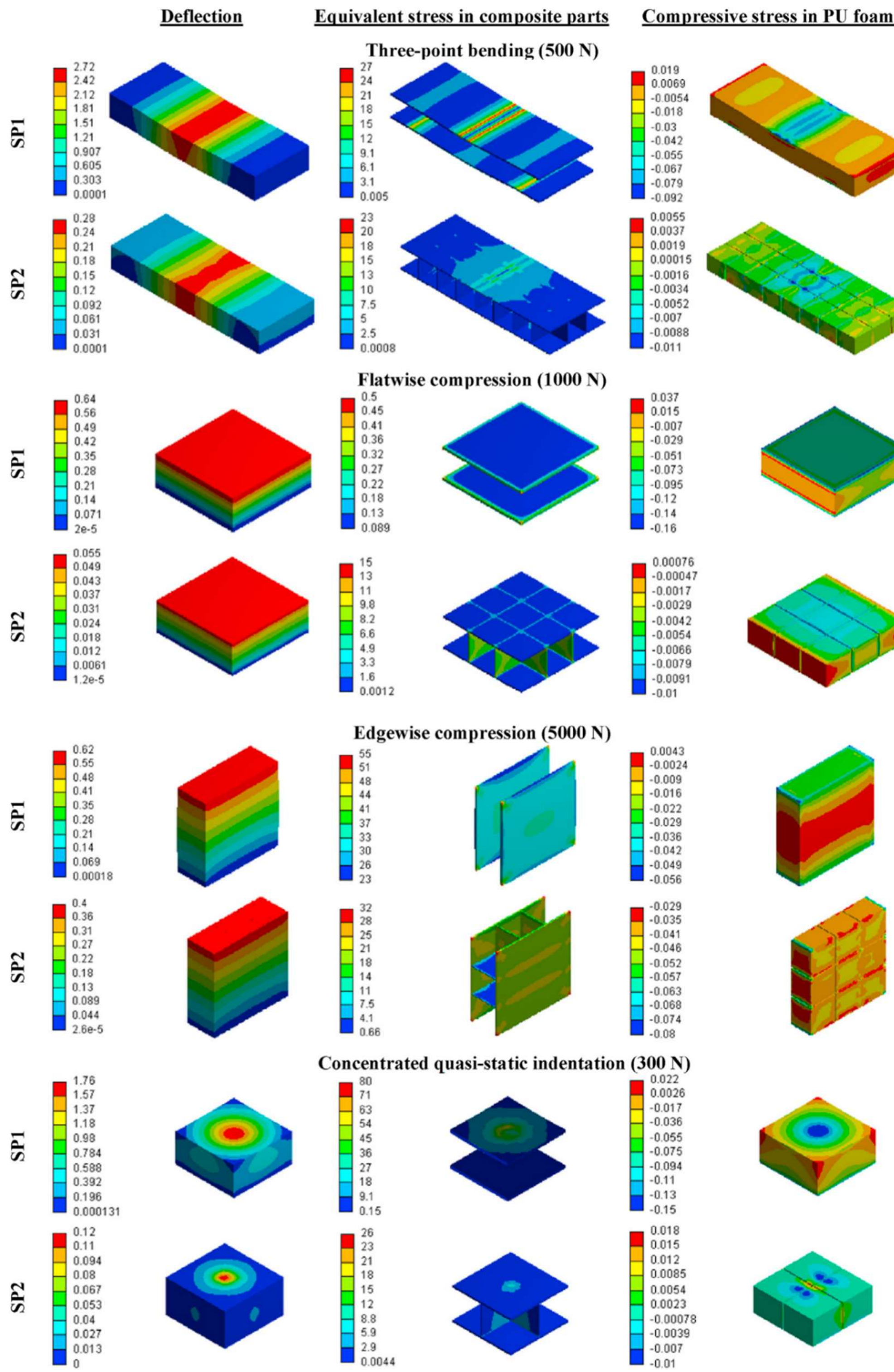

Fig. 25. The distribution contours of deformation, equivalent stress in composite parts, and compressive stress in core for SP1 and SP2 specimens under different loading conditions.

As can be seen in Fig. 25 and Table 9, applying the load of 500 N resulted in a maximum deflection of 2.72 mm and 0.28 mm in mid-span of SP1 and SP2 specimens, respectively. The maximum deflection values obtained from the experimental tests were about 2.81 mm and 0.33 mm for SP1 and SP2 specimens, respectively. Therefore, it was concluded that under the same applied load (500 N), the maximum deflection exhibited by SP1 specimen was numerically and experimentally 871% and 907% higher than that of SP2 specimen, respectively. The FE models also predicted the maximum deflection of 0.64, 0.62, and 1.76 mm for SP1 specimens, which was 1180%, 55%, and 1367% higher than those measured for SP2 specimens.

Equivalent stress distribution contours in composite parts including skins and lattice structure and their associated values are shown in Fig. 25 and Table 9. Similar to those observed in the experimental findings, the location of stress concentration was well predicted in the specimens. The examination of maximum equivalent stress values indicates that the utilization of the thin-walled lattice structure could successfully decrease the equivalent stress in composite parts. Since composite skins tolerated no significant portion of compressive load in SP1 configuration under flatwise compressive loading, the proposed structural modifications led to a reduction of compressive stress in PU foam.

Considering the multilayered nature of core in SP2 specimens (i.e. hybrid of agglomerated cork and PU foam), to make a completely identical comparison, the maximum compressive stress is presented only for the PU part of the core. It can be clearly observed from Fig. 25 and Table 9 that the proposed structural modifications could significantly decrease the maximum compressive stress value in the PU foam from 0.09 to 0.01 MPa, 0.16 to 0.01 MPa, and 0.15 to 0.01 MPa, under bending, flatwise compressive, and indentation loads, respectively. Only a slight increase in maximum compressive stress from 0.06 to 0.08 MPa was observed in the compressed state. Therefore, it can be concluded that the utilization of a thin-walled lattice structure within the sandwich structure could effectively relieve the stress in core and hinder the PU foam from premature cracking and crushing. Furthermore, the agglomerated cork layers as an intermediate layer with moderate properties were most likely able to prevent the sudden transfer of stress from the skin to PU foam core by withstanding a significant amount of applied load.

5. Conclusions

In this work, a novel sandwich panel based on a multilayered hybrid core stiffened by a composite lattice structure and two composite skins was successfully designed and manufactured. The core was made of agglomerated cork and polyurethane (PU) foam, and epoxy/E-glass fiber laminates were used to manufacturing all composite parts. The effectiveness of this novel sandwich system (SP2) compared to the traditional PU foam-cored sandwich panels (SP1) was investigated by a series of experimental tests including water immersion conditioning, three-point bending, edgewise and flatwise compression, quasi-static indentation, and high-velocity impact perforation. The structural responses of two studied sandwich systems were also numerically examined using finite element (FE) analysis. From the experimental and numerical results, the following important conclusions can be drawn:

1. The maximum level of water uptake recorded for multilayered hybrid specimens i.e. PU foam/agglomerated cork (PU/C/S) was less than half of the water uptake in monolithic PU foam (PU/S) specimens, indicating the superior barrier role of agglomerated cork layers against the water penetration within the structure.
2. Without any increase in weight, the maximum flexural load, initial flexural stiffness, and flexural toughness of the SP2 specimens improved by 506%, 816%, and 145% respectively, in comparison to the SP1 specimens.

3. The examination of failure modes revealed that utilization of a thin-walled lattice structure could significantly enhance the structural performance of the SP2 system in several effective ways, as follows:
    - Improved delamination resistance by decreasing the shear stress level in core-skin interfacial bonding;
    - Enhanced compressive stiffness and strength of the core and delayed foam crushing by supporting the core in through-thickness direction;
    - Improved stress distribution and subsequently increased load carrying capacity of structure through connecting the top and bottom skins.
4. The results of the flatwise compression tests showed that compared to the SP1 specimens, an increase of about 2080% and 1233% in the maximum compressive load and compressive stiffness could be achieved through the proposed modifications made in SP2 systems.
5. Edgewise compression tests revealed that the maximum compressive load and compressive stiffness of SP2 sandwich systems are approximately 47% and 8%, respectively, higher than those offered by the SP1 systems. This less significant improvement in edgewise mode was attributed to the natural structural response of sandwich panels to this type of loading, where unlike the flatwise mode, both the core and skins contribute in the load-bearing process.
6. It was found that the synergistic effect of energy-absorbent cork layer sand stiff composite lattice structure in SP2 specimens could dramatically increase both the quasi-static indentation and high-velocity impact perforation behavior of PU foam-cored sandwich panels. The SP2 specimens showed an improvement of about 794%, 1274%, and 21% in maximum indentation load, indentation stiffness, and absorbed impact energy over SP1 specimens, respectively. It was shown that both the above-mentioned loading types could

almost similarly affect the specimens in terms of failure modes. It was also found that neither indenter in quasi-static mode nor projectile in high-velocity regime could fully penetrate the rear side of SP2 specimens. This indicates superior damage tolerance and energy absorption of these novel sandwich systems.

7. The nonlinear FE results successfully indicated the proposed structural modifications could effectively enhance the structural performance of traditional PU foam cored-sandwich panels. It was also found that the proposed FE model could reasonably predict the structural performance of studied sandwich systems, especially in the linear-elastic regime. Therefore, this model can be used at the preliminary design stage.

The finding of this feasibility study can provide a new opportunity to introduce a novel sandwich system for use in marine sectors while preserving superior mechanical properties, low-weight, and environmental durability requirements.

Declaration of competing interest

The authors declare that they have no known competing financial interests or personal relationships that could have appeared to influence the work reported in this paper.

References

[1] C. Borsellino, L. Calabrese, G. Di Bella, Effect of bonder at skin/core interface on the mechanical performances of sandwich structures used in marine industry, Appl. Compos. Mater. 14 (2007) 307-323.

[2] G. Palomba, V. Crupi, G. Epasto, Collapse modes of aluminium honeycomb sandwich structures under fatigue bending loading, Thin-Walled Struct. 145 (2019) 106363.

[3] D. Zenkert, The Handbook of Sandwich Construction, first ed., Engineering Materials Advisory Services Ltd, London, 1997.

[4] V. Crupi, E. Kara, G. Epasto, E. Guglielmino, H. Aykul, Prediction model for the impact response of glass fibre reinforced aluminium foam sandwiches, Int. J. Impact Eng. 77 (2015) 97-107.

[5] T. Lanssens, Ch Tanghe, N. Rahbar, P. Okumus, S. Van Dessel, T. El-Korchi, Mechanical behavior of a glass fiber-reinforced polymer sandwich panel with through-thickness fiber insertions, Construct. Build. Mater. 64 (2014) 473-479.

[6] L. Wang, W. Liu, L. Wan, H. Fang, D. Hui, Mechanical performance of foam-filled lattice composite panels in four-point bending: experimental investigation and analytical modeling, Compos. B Eng. 67 (2014) 270-279.

[7] J. Tao, F. Li, D. Zhang, J. Liu, Z. Zhao, Manufacturing and mechanical performances of a novel foam core sandwich-walled hollow column reinforced by stiffeners, ThinWalled Struct. 139 (2019) 1-8.

[8] S. Sayahlatifi, G.H. Rahimi, A. Bokae, Experimental and numerical investigation of sandwich structures with balsa core and hybrid corrugated composite/balsa core under three-point bending using digital image correlation, J. Sandw. Struct. Mater. (2019), https://doi.org/10.1177/1099636218822333.

[9] K. Branner, Capacity and Lifetime of Foam Core Sandwich Structures, Ph.D. Thesis, Technical University of Denmark, 1995.

[10] C. Atas, C. Sevim, On the impact response of sandwich composites with cores of balsa wood and PVC foam, Compos. Struct. 93 (1) (2010) 40-48.

[11] M. Osei-Antwi, J. De Castro, A.P. Vassilopoulos, T. Keller, Shear mechanical characterization of balsa wood as core material of composite sandwich panels, Construct. Build. Mater. 41 (2013) 231-238.

[12] C. De Marco Muscat-Fenech, J. Cortis, C. Cassar, Impact damage testing on composite marine sandwich panels, part 1: quasi-static indentation, J. Sandw. Struct. Mater. 16 (5) (2014) 443-480.

[13] B. Hayman, A.T. Echtermeyer, Reduction of strength of GFRP sandwich panels in naval ships by face sheet holes, cracks and impact damage, J. Sandw. Struct. Mater. 21 (5) (2019) 1621-1653.

[14] Z. Huo, M. Mohamed, J.R. Nicholas, S. Anandan, K. Chandrashekhara, Effect of salt water exposure on foam-cored polyurethane sandwich composites, J. Sandw. Struct. Mater. 22 (4) (2010) 1256-1273.

[15] B. Koohbor, A. Kidane, Design optimization of continuously and discretely graded foam materials for efficient energy absorption, Mater. Des. 102 (2016) 151-161.

[16] M.S. Mohammadi, J.A. Nairn, Crack propagation and fracture toughness of solid balsa used for cores of sandwich composites, J. Sandw. Struct. Mater. 16 (1) (2014) 22-41.

[17] N. Dimitrov, C. Berggreen, Probabilistic fatigue life of balsa cored sandwich composites subjected to transverse shear, J. Sandw. Struct. Mater. 17 (5) (2015) 562-577.

[18] M. Najafi, R. Ansari, A. Darvizeh, Experimental characterization of a novel balsa cored sandwich structure with fiber metal laminate skins, Iran, Polym. J. 28 (2019) 87-97.

[19] D.R. Veazie, K.R. Robinson, K. Shivakumar, Effects of the marine environment on the interfacial fracture toughness of PVC core sandwich composites, Compos. B Eng. 35 (6-8) (2004) 461-466.

[20] F. Aviles, M. Aguilar-Montero, Mechanical degradation of foam-cored sandwich materials exposed to high moisture, Compos. Struct. 92 (1) (2010) 122-129.

[21] B.J. Manujesh, R. Vijayalakshmi, M.P. Sham, Moisture absorption and mechanical degradation studies of polyurethane foam cored E-glass-reinforced vinyl-ester sandwich composites, J. Reinforc. Plast. Compos. 33 (5) (2014) 479-492.

[22] Z. Xue, Z. Hu, H. Gao, P. Hu, Evaluation study on composite hull structure subjected to slamming loads, in: 18th International Conference on Composite Materials, Jeju Island, Korea, 2011.

[23] B. Lascoup, Z. Aboura, K. Khellil, M. Benzeggagh, On the mechanical effect of stitch addition in sandwich panel, Compos. Sci. Technol. 66 (10) (2006) 1385-1398.

[24] P. Potluri, E. Kusak, T.Y. Reddy, Novel stitch-bonded sandwich composite structures, Compos. Struct. 59 (2) (2003) 251-259.

[25] A. Nanayakkara, S. Feih, A.P. Mouritz, Experimental analysis of the through the thickness compression properties of z pinned sandwich composites, Compos. Part A Appl. Sci. Manuf. 42 (11) (2011) 1673-1680.

[26] A. Marasco, D.D. Cartie, I. Partridge, A. Rezai, Mechanical properties balance of novel z-pinned sandwich panel: out-of-plane properties, Compos. Part A Appl. Sci. Manuf. 37 (2) (2006) 295-302.

[27] N. Mitra, A methodology for improving shear performance of marine grade sandwich composites: sandwich composite panel with shear key, Compos. Struct. 92 (5) (2010) 1065-1072.

[28] A. Mostafa, K. Shankar, E.V. Morozov, In-plane shear behaviour of composite sandwich panel incorporated with shear keys methodology at different orientations: finite element study, J. Compos. Mater. 48 (24) (2014) 2945-2959.

[29] H. Tuwair, M. Hopkins, J. Volz, M.A. ElGawady, M. Mohamed, K. Chandrashekhara, V. Birmand, Evaluation of sandwich panels with various polyurethane foam-cores and ribs, Compos. B Eng. 79 (2015) 262-276.

[30] J. Zhou, Z.W. Guan, W.J. Cantwell, Y. Liao, The energy absorbing behavior of foam cores reinforced with composite rods, Compos. Struct. 116 (2014) 346-356.

[31] B. Lascoup, Z. Aboura, K. Khellil, M. Benzeggagh, Homogenization of the core layer in stitched sandwich structures, Compos. Sci. Technol. 70 (2) (2010) 350-355.

[32] H.E. Yalkin, B.M. Icten, T. Alpyildiz, Enhanced mechanical performance of foam core sandwich composites with through the thickness reinforced core, Compos. B Eng. 79 (2015) 383-391.

[33] Y. Zheng, J. Xiao, M. Duan, L. Yong, Experimental study of partially-cured Z-pins reinforced foam core composites: K-Cor sandwich structures, Chin. J. Aeronaut. 27 (1) (2014) 153-159.

[34] S.A. Taghizadeh, A. Farrokhabadi, Gh Liaghat, E. Pedram, H. Malekinejad, Characterization of compressive behavior of PVC foam infilled composite sandwich panels with different corrugated core shapes, Thin-Walled Struct. 135 (2019) 160-172.

[35] C. Kaboglu, L. Yu, I. Mohagheghian, Effects of the core density on the quasi-static flexural and ballistic performance of fibre-composite skin/foam core sandwich structures, J. Mater. Sci. 53 (24) (2018) 16393-16414.

[36] M. Najafi, A. Darvizeh, R. Ansari, Characterization of moisture effects on novel agglomerated cork core sandwich composites with fiber metal laminate facesheets, J. Sandw. Struct. Mater. 22 (6) (2020) 1709-1742.

[37] D. Li, Z. Deng, H. Xiao, P. Jin, Bending analysis of sandwich plates with different face sheet materials and functionally graded soft core, Thin-Walled Struct. 122 (2018) 8-16.

[38] Datasheet/Corecork NL10, 2017, https://amorimcorkcomposites.com/en-us/ downloads/.

[39] ASTM D1621, Standard Test Method for Compressive Properties of Rigid Cellular Plastics, American Society for Testing and Materials, West Conshohocken, Pennsylvania, 2016.

[40] ASTM D3039/D3039M, Standard Test Method for Tensile Properties of Polymer Matrix Composite Materials, American Society for Testing and Materials, West Conshohocken, Pennsylvania, 2016.

[41] ASTM C393/C393M, Standard Test Method for Core Shear Properties of Sandwich Constructions by Beam Flexure, American Society for Testing and Materials, West Conshohocken, Pennsylvania, 2011.

[42] ASTM C365/C365M, Standard Test Method for Flatwise Compressive Properties of Sandwich Cores, American Society for Testing and Materials, West Conshohocken, Pennsylvania, 2016.

[43] ASTM C364, Standard Test Method for Edgewise Compressive Strength of Sandwich Constructions, American Society for Testing and Materials, West Conshohocken, Pennsylvania, 1999.

[44] ASTM D7766/D7766M, Standard Practice for Damage Resistance Testing of Sandwich Constructions, American Society for Testing and Materials, West Conshohocken, Pennsylvania, 2016.

[45] E. Sevkat, B. Liaw, F. Delale, B.B. Raju, Drop-weight impact of plain-woven hybrid glass-graphite/toughened epoxy composites, Compos. Part A Appl. Sci. Manuf. 40 (2009) 1090-1110.

[46] R.M. Jones, Mechanics of Composite Materials, second ed., Taylor & Francis Ltd., London, 1999.

[47] S.Z. Sheng, S. Van Hoa, Three dimensional micro-mechanical modeling of woven fabric composites, J. Compos. Mater. 35 (19) (2001) 1701-1729.

[48] S.P. Silva, M.A. Sabino, E.M. Fernandes, V.M. Correlo, L.F. Boesel, R.L. Reis, Cork: properties, capabilities and applications, Int. Mater. Rev. 50 (6) (2005) 345-365.

[49] M. Szycher, Szycher'S Handbook of Polyurethanes, second ed., Taylor & Francis Ltd., London, 2013.

[50] S. Lequin, D. Chassagne, T. Karbowiak, J.M. Simon, C. Paulin, J.P. Bellat, Diffusion of oxygen in cork, J. Agric. Food Chem. 60 (13) (2012) 3348-3356.

[51] T. Karbowiak, R.D. Gougeon, J.B. Alinc, L. Brachais, F. Debeaufort, A. Voilley, D. Chassagne, Wine oxidation and the role of cork, Crit. Rev. Food Sci. Nutr. 50 (1) (2010) 20-52.

[52] L.J. Gibson, M.F. Ashby, Cellular Solids: Structure and Properties, second ed., Cambridge University Press, Cambridge, 1999.

[53] H.E. Yalkin, B.M. Icten, T. Alpyildiz, Tensile and compressive performances of foam core sandwich composites with various core modifications, J. Sandw. Struct. Mater. 19 (1) (2017) 49-65.

[54] V.G.K. Menta, R.R. Vuppalapati, K. Chandrashekhara, D. Pfitzinger, N. Phan, Manufacturing and mechanical performance evaluation of resin-infused honeycomb composite Materials, J. Reinforc. Plast. Compos. 31 (6) (2012) 415-423.

[55] H. Khosravi, R. Eslami-Farsani, Reinforcing effect of surface-modified multiwalled carbon nanotubes on flexural response of E-glass/epoxy isogrid-stiffened composite panels, Polym. Compos. 39 (S2) (2018) E677-E686.

[56] L. Gil, Cork composites: a review, Materials 2 (3) (2009) 776-789.

[57] O. Castro, J.M. Silva, T. Devezas, A. Silva, L. Gil, Cork agglomerates as an ideal core material in lightweight structures, Mater. Des. 31 (1) (2010) 425-432.